ISSN : 2311-5122

7universum.com

UNIVERSUM: ТЕХНИЧЕСКИЕ НАУКИ

9(150)

НАУЧНЫЙ ЖУРНАЛ

...са́ндрович Попо́в (1821, Санкт-Петербург — ... Петербург) — русский флотоводец, ...роитель, адмирал (1891 год). Его имя носит ... Попова рядом с Владивостоком.
Родился 22 сентября (4 октября) 1821 года в Санкт-Петербурге в семье известного кораблестроителя, управляющего Охтинской верфью Александра Андреевича Попова.

С 1830 года учился на морском отделение Александровского корпуса; в 1838 году окончил Морской кадетский корпус с присвоением чина мичмана и зачислением в 32-й флотский экипаж (Черноморский флот).

был командиром парохода «Метеор» (вспомогательного крейсера Черноморского флота). В 1853 году был командирован в Константинополь для сбора сведений о вооружении Босфора и близлежащих к нему укреплённых мест по Чёрному морю и Дунаю до Рущука. Участвовал в Крымской кампании. В 1853—1854 годах командовал пароходами «Эльборус», «Андия», «Турок», потопил шесть турецких транспортов; в сентябре 1854 года командовал в чине капитан-лейтенанта пароходом «Тамань», прорвался из блокированного Севастополя в Одессу и вернулся обратно с грузом для оборонявшихся.

Руководил установкой морских орудий на укреплениях Севастополя и артиллерийским снабжением. Руководил снаряжением двух брандеров. Руководил созданием бона для преграждения севастопольского рейда. За боевые заслуги в этот период — награждён двумя орденами.

Произведен в капитаны 1-го ранга; с 1855 — флигель-адъютант. В 1855 году был командирован с театра военных действий в Кронштадт, Выборг, Свеаборг и другие укреплённые порты побережья Балтийского моря. В период 1856—1858 годов был начальником штаба Кронштадтского порта.

В 1858—1861 гг. — командующий отрядом из двух корветов («Рында» и «Гридень») и клипера ... (2-й Амурский отряд), приведя его из Кронштадта в Японское море, затем ходил у берегов Японии, исследовал побережья русского Приморья (один из заливов — у 45-й параллели — был назван ... корвета Попова «Рында»). В 1859 году ... командованием нанесли визит в порт Сан-Фр...

205 ЛЕТ СО ДНЯ РОЖДЕНИЯ

21 сентября 2026 г.

ПОПОВ
АНДРЕЙ АЛЕКСАНДРОВИЧ
1821-1898 гг.

РУССКИЙ ФЛОТОВОДЕЦ, КОРАБЛЕСТРОИТЕЛЬ, АДМИРАЛ

Г. МОСКВА

7universum.com
UNIVERSUM:
ТЕХНИЧЕСКИЕ НАУКИ

UNIVERSUM: ТЕХНИЧЕСКИЕ НАУКИ

Научный журнал

Издается ежемесячно с ноября 2013 года

Выпуск: 9(150)

Сентябрь 2026 г.

Часть 8

Новосибирск
2026

ББК 3
U55

U55 Universum: технические науки : электронный научный журнал. — № 9(150). — Часть 8. — Новосибирск : Изд-во «Юниверсум», 2026. — 68 с. — Текст : электронный. — URL: https://7universum.com/ru/tech/archive/category/9150 (дата публикации: 28.09.2206).

ISSN 2311-5122
DOI: 10.32743/UniTech.2026.150.9
Учредитель и издатель: ООО «Юниверсум»

Содержание

ARTICLES IN ENGLISH

INDUSTRY AND MANUFACTURING

TEXTILE AND LIGHT INDUSTRY

Статья поступила в редакцию: 11.09.2026
Статья принята к публикации: 19.09.2026
Статья опубликована: 28.09.2206

УДК 677.025

DOI: 10.32743/UniTech.2026.150.9.23444

Influence of elastane yarn distribution on the technological properties of fleece knitted fabrics

Boqirboyev Foziljon Rasuljon ugli
Researcher
Namangan davlat texnika universiteti
Uzbekistan, Namangan

Shogofurov Shakhboz Shokirjon ugli
PhD
Namangan davlat texnika universiteti
Uzbekistan, Namangan
E-mail: shogofurov@mail.ru

Библиографическое описание: Бокирбоев Ф.Р.У., Шогофуров Ш.Ш.У. Влияние распределения эластановой пряжи на технологические свойства трикотажных тканей флиса // Universum: технические науки : электрон. научн. журн. 2026. 9(150). URL: https://7universum.com/ru/tech/archive/item/23444

For citation: Boqirboyev F.R.U., Shogofurov S.S.U. Influence of elastane yarn distribution on the technological properties of fleece knitted fabrics // Universum: Technical Sciences : electronic scientific journal. 2026. No. 9(150). Available at: https://7universum.com/ru/tech/archive/item/23444

Влияние распределения эластановой пряжи на технологические свойства трикотажных тканей флиса

Бокирбоев Фозилжон Расулжон угли
Исследователь Наманганский давлатский технологический университет
Республика Узбекистан, г. Наманган

Шогофуров Шахбоз Шокиржон угли
д-р филос. Наманганский давлатский технологический университет
Республика Узбекистан, г. Наманган

Abstract

This study investigates the effect of the amount of elastane yarn and its distribution sequence within the structure of weft-knitted fleece fabric on its technological and geometrical characteristics. Experimental studies were carried out using spun cotton yarn and highly elastic elastane yarn on a single-bed Wellknit knitting machine. Five variants of fleece knitted fabrics were developed, differing in the elastane yarn content and its distribution across the fabric courses. During the experiments, the main geometrical and physical parameters of the produced samples were determined and comparatively analyzed, including loop pitch, course height, horizontal and vertical density, yarn length consumed per loop, areal density, thickness, and bulk density. Changes in these parameters were evaluated in relation to the elastane yarn content and its arrangement within the fabric repeat. The experimental results demonstrated that both the proportion of elastane yarn and its distribution pattern within the repeat have a significant effect on the structural parameters of fleece knitted fabrics. In particular, the sample containing elastane yarn in all courses exhibited increased horizontal and vertical density, accompanied by greater fabric thickness and a higher tendency toward elastic deformation. Although variants III, IV, and V showed relatively high thickness values, they demonstrated acceptable bulk density and raw material consumption characteristics..

Аннотация

Данное исследование изучает влияние количества эластановой пряжи и последовательности её распределения в структуре уточно-вязаной ткани флиса на её технологические и геометрические характеристики. Экспериментальные исследования проводились с использованием пряжи из кардного хлопка и высокоэластичной эластановой пряжи на одноигольной вязальной машине Wellknit. Разработано пять вариантов трикотажных тканей флиса, отличающихся содержанием эластановой пряжи и её распределением по рядам ткани. При проведении экспериментов определены и сравнительно проанализированы основные геометрические и физические параметры полученных образцов, включая шаг петли, высоту ряда, горизонтальную и вертикальную плотность, длину пряжи, расходуемую на одну петлю, поверхностную плотность, толщину и объёмную плотность. Изменения указанных параметров оценивались в зависимости от содержания эластановой пряжи и её размещения в пределах раппорта ткани. Результаты экспериментов показали, что как доля эластановой пряжи, так и её схема распределения в пределах раппорта оказывают значительное влияние на структурные параметры трикотажных тканей флиса. В частности, образец, содержащий эластановую пряжу во всех рядах, продемонстрировал повышенные

горизонтальную и вертикальную плотность, сопровождаемые большей толщиной ткани и более высокой склонностью к упругой деформации. Хотя варианты III, IV и V показали относительно высокие значения толщины, они продемонстрировали приемлемые объёмную плотность и характеристики расхода сырья.

Keywords: elastane yarn, knitted fabric structure, loop pitch, fabric density, areal density, thickness, bulk density.

Ключевые слова: эластановая пряжа, структура трикотажной ткани, шаг петли, плотность ткани, поверхностная плотность, толщина, объёмная плотность.

Introduction

Fleece knitted fabrics are among the widely used knitted materials in the modern textile industry, and their structural characteristics and technological parameters are important factors determining the quality and functional performance of finished products [1; 26-28 p, 2; 329-351 p]. Parameters such as loop pitch, course height, horizontal and vertical density, areal density, and thickness affect not only the stability of the fabric formation process but also the fit, comfort, and appearance retention of products manufactured from these fabrics [3; 352-365 p].

Spun cotton yarn is widely used as the primary raw material in the production of conventional fleece knitted fabrics. The hygienic properties, moisture absorption capacity, and consumer-related characteristics of cotton fibers make them suitable for such products. The incorporation of elastane yarn into the fabric structure can affect the geometrical configuration of loop elements, their mutual arrangement, the degree of fabric compaction, and the overall structure of the fabric in its relaxed state [4; 463-479 p].

In addition to the amount of elastane yarn, its distribution within the fabric structure is an important technological factor in determining the final properties of fleece knitted fabrics. The placement of elastane yarn in the plain or fleece courses, as well as its repetition according to a specific sequence within the fabric repeat, alters the conditions under which the loop elements are formed [5; 741-754 p, 6; 310-319 p].

Studies aimed at optimizing the technological parameters of knitted fabrics consider the combined effects of factors such as raw material type, yarn linear density, yarn length per loop, machine operating conditions, interaction between the needle beds, and fabric structure as important research variables [7; 1-7 p, 8; 1-11 p].

The aim of this study is to develop different variants of fleece knitted fabrics using spun cotton yarn and elastane yarn and to determine the effect of the amount and distribution of elastane yarn within the fabric structure on key technological parameters, including loop pitch, horizontal and vertical density, areal density, thickness, and bulk density.

Materials

The effect of elastane yarn on the technological and physical-mechanical properties of knitted fabric was studied at the “Terry Jar” enterprise, with particular attention to determining its appropriate content. The experiments were carried out on a single-bed Wellknit knitting machine. Spun cotton yarn of 20 tex and highly elastic elastane yarn of 7.7 tex were used for producing the

experimental samples. During the experimental study, five variants of fleece knitted fabric were produced. All samples were knitted under identical technological conditions; the machine settings, yarn tension, and production speed were kept constant throughout the process. The samples differed only in the amount of elastane yarn incorporated into the fabric and its arrangement within the structure. This approach allowed the obtained results to be compared accurately and reliably [9; 1-7 p].

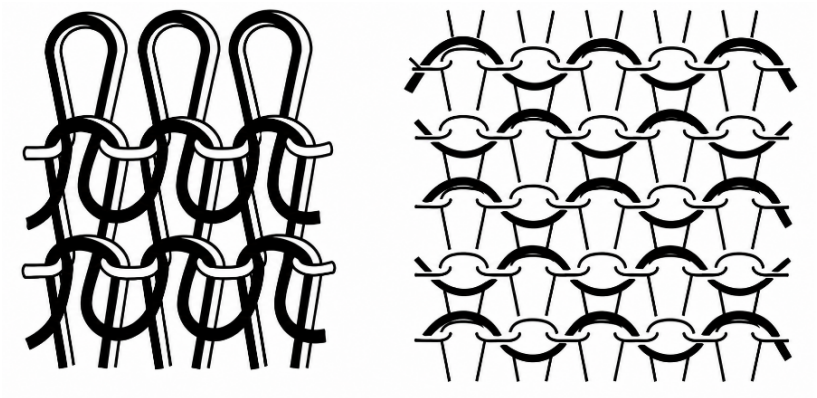

Figure 1. Loop structure and arrangement of loop elements in fleece knitted fabric

Figure 1 presents the graphical notation of the produced fleece knitted fabric sample. It provides a basis for analyzing the structural elements of the fabric, their arrangement, and the patterns of their interconnection in detail [10; 1-8 p].

In Variant I, the fabric repeat consisted of two courses. The first was a plain course knitted using spun cotton yarn combined with elastane yarn. The second was a fleece course formed exclusively from spun cotton yarn. Variant II also consisted of a two-course repeat. The first plain course was knitted from spun cotton yarn. In the second course, elastane yarn was combined with spun cotton yarn as the ground yarn, while only spun cotton yarn was used as the fleece yarn. In Variant III, the repeat likewise consisted of two courses. The first plain course was knitted from a combination of spun cotton and elastane yarns. In the second course, spun cotton yarn combined with elastane yarn was used as the ground yarn, while spun cotton yarn was used as the fleece yarn. In Variant IV, the repeat was composed of four courses. The first and second courses were knitted from spun cotton yarn. In the third course, spun cotton yarn was combined with elastane yarn. In the fourth course, spun cotton and elastane yarns were used together as the ground yarn, while spun cotton yarn was used as the fleece yarn. Variant V also had a four-course repeat. The first course was a plain course knitted from spun cotton yarn. In the second and fourth courses, spun cotton yarn combined with elastane yarn was used as the ground yarn, while spun cotton yarn served as the fleece yarn. The third course was a plain course knitted from a combination of spun cotton and elastane yarns. In this variant, elastane yarn was distributed more uniformly throughout the repeat, which was intended to provide a balanced combination of fabric elasticity and shape retention.

Results and Discussion

The linear densities of the yarns used in the fleece knitted fabrics and their proportions in the fabric are presented in Table 1.

Table 1.

Technological parameters of fleece knitted fabric

Parameter	I	II	III	IV	V
Raw material type and proportion in the fabric, % (fleece/ground/elastane)	54.8/45.2/-	51.4/44.6/4	50.8/44.9/4.3	53/43.2/3.8	51/44.4/4.6
Loop pitch A, mm	0.74	0.72	0.69	0.71	0.71
Course height V, mm	0.63	0.63	0.61	0.65	0.62
Horizontal density Rg	68	69	72	70	70
Vertical density Rv	79	79	82	77	81
Yarn length per loop, mm	6.1	6.5	5.9	6	6.1
Fabric areal density Ms, g/m²	262	283	279	259	277
Thickness T, mm	1.15	1.35	1.3	1.22	1.27
Bulk density δ, mg/cm³	228	210	214	212	218

The data given in Table 1 indicate that the introduction of 3.8–4.6 % elastane yarn into the fleece knitted fabric changes its technological parameters in a consistent manner. One of the most noticeable changes is the reduction in loop pitch with increasing elastane content. This behavior is associated with the elastic recovery of the yarn. Once the fabric is removed from the knitting machine and reaches a relaxed state, the elastane yarn contracts and pulls the adjacent loops closer together. As a result, the distance between the loops decreases and the knitted structure becomes more compact

The areal density of the fleece knitted fabrics is closely associated with the repeat structure and the amount of elastane yarn incorporated into the fabric. The relationship between these parameters is illustrated graphically in Figure 2.

The experimental results further demonstrate that both areal density and thickness vary according to the amount and distribution of elastane yarn within the fabric structure. A comparison of Variants I and II shows that the areal density increases from 262 to 283 g/m², corresponding to an increase of approximately 8.0 %. Fabric thickness also rises from 1.15 to 1.35 mm. This increase can be attributed to the contraction of elastane yarn and the resulting rearrangement and compaction of the loop structure when the fabric reaches its relaxed state. The incorporation of elastane yarn into the fleece course therefore affects not only the density of the fabric but also its thickness and overall structural configuration.

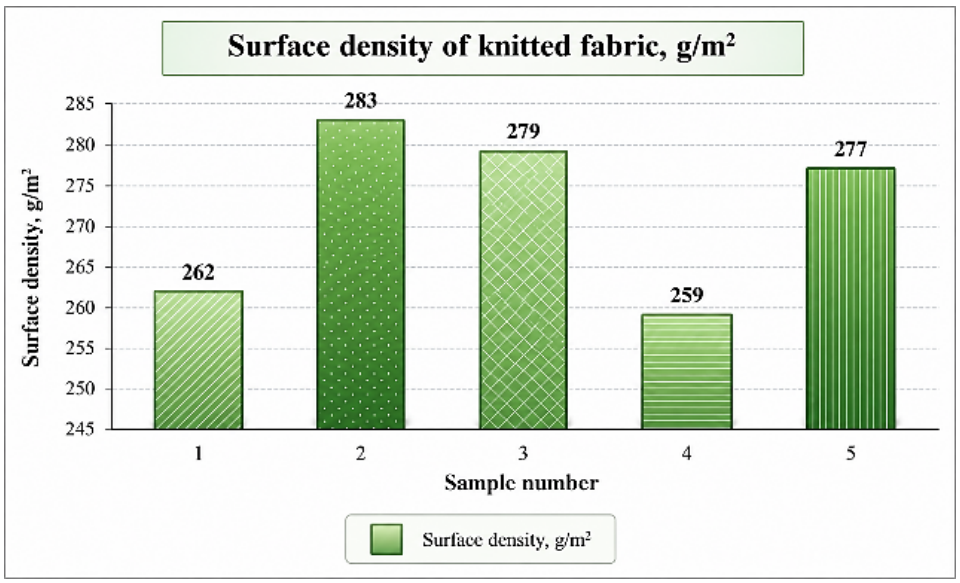

Figure 2. Diagram of changes in the areal density of fleece knitted fabric

Variant III, in which elastane yarn was incorporated into all courses, showed the highest areal density and thickness values among the investigated samples. This suggests that the more uniform distribution of elastane yarn throughout the fabric structure promotes greater structural compaction and affects the elastic behavior of the knitted fabric.

The bulk density of Variant II was 1.9 % lower than that of Variant I. Similarly, the bulk density of Variant IV was lower than that of Variant V. According to the values presented in Table 1, these parameters were 212 and 218 mg/cm³, respectively, corresponding to a difference of approximately 2.8 %. The lowest bulk density was observed in Variant II, at 210 mg/cm³, rather than in Variant III. This indicates that the increase in fabric thickness in Variant II was accompanied by a relatively lower increase in areal density, resulting in a lower overall bulk density and a more open internal structure.

The bulk density values of the investigated knitted fabric samples ranged from 210 to 228 mg/cm³, as shown graphically in Figure 3. The obtained results demonstrate that both the amount of elastane yarn and its distribution within the knitted structure influence not only fabric density and thickness but also its bulk characteristics, including lightness, internal porosity, and the efficiency of raw material utilization.

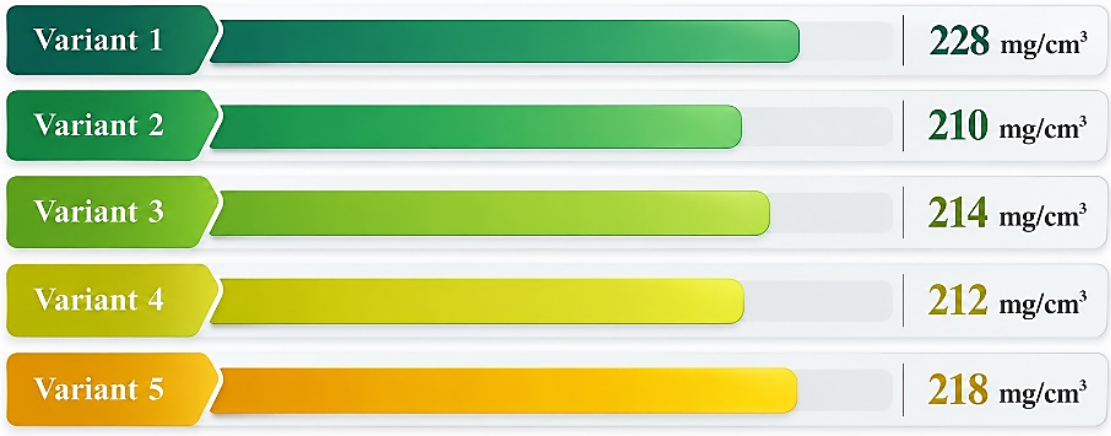

Figure 3. Raw material consumption of fleece knitted fabrics

Conclusion

The experimental results demonstrate that both the content and distribution of elastane yarn within the repeat have a substantial effect on the structural and technological characteristics of fleece knitted fabrics. Increasing the elastane content and modifying its position within the repeat altered the loop pitch, horizontal and vertical density, areal density, thickness, and bulk density of the fabrics. The incorporation of elastane yarn promoted structural compaction and elastic recovery of the knitted fabric after its removal from the machine. At the same time, differences in elastane distribution produced distinct changes in fabric thickness and bulk characteristics. Among the investigated samples, Variants III, IV, and V demonstrated a favorable combination of thickness, bulk density, and material consumption. These results indicate that rational distribution of elastane yarn can be used to regulate the structure of fleece knitted fabrics and obtain products with an appropriate balance between material efficiency, lightweight construction, thickness, elasticity, and shape retention.

References

1. Spencer D.J. Knitting Technology: A Comprehensive Handbook and Practical Guide. – 3rd ed. – Cambridge: Woodhead Publishing, 2001. – 416 P.
2. Postle R. Analysis of the Dry-Relaxed Knitted-Loop Configuration: Part I: Two-Dimensional Analysis / R. Postle, D.L. Munden // The Journal of the Textile Institute. – 1967. – Vol. 58, No. 8. – P. 329–351. – DOI: 10.1080/00405006708629880.
3. Postle R. Analysis of the Dry-Relaxed Knitted-Loop Configuration: Part II: Three-Dimensional Analysis / R. Postle, D.L. Munden // The Journal of the Textile Institute. – 1967. – Vol. 58, No. 8. – P. 352–365. – DOI: 10.1080/00405006708629881.
4. Eryuruk S.H. Analysis of the performance properties of knitted fabrics containing elastane / S.H. Eryuruk, F. Kalaoglu // International Journal of Clothing Science and Technology. – 2016. – Vol. 28, No. 4. – P. 463–479. – DOI: 10.1108/IJCST-10-2015-0120.
5. Strength, fatigue and bagging properties of plated plain knitted fabrics containing different rates of elastane // International Journal of Clothing Science and Technology. – 2019. – Vol. 31, No. 6. – P. 741–754. – DOI: 10.1108/IJCST-10-2018-0129.
6. Schwartz P. Structure and mechanics of textile fibre assemblies / P. Schwartz (Ed.). – Cambridge: Woodhead Publishing, 2019. – 370 P.
7. Eltahan E. Effect of Lycra Percentages and Loop Length on the Physical and Mechanical Properties of Single Jersey Knitted Fabrics // Journal of Composites. – 2016. – Art. 3846936. – DOI: 10.1155/2016/3846936.
8. Ivanovska A. Studying the influence of common wet processes on the quality of 1 × 1 rib cotton/elastane knitted fabrics / A. Ivanovska [et al.] // Journal of Engineered Fibers and Fabrics. – 2022. – Vol. 17. – P. 1–11. – DOI: 10.1177/15589250221145522.
9. Shogofurov S. Mathematical modeling of the elongation of a knitted fabric / S. Shogofurov [et al.] // AIP Conference Proceedings. – 2023. – Vol. 2789, No. 1. – Art. 040131. – P. 1–7. – DOI: 10.1063/5.0145479.

10. Shogofurov S. Complex evaluation diagram of backed knitted fabric / S. Shogofurov [et al.] // AIP Conference Proceedings. – 2023. – Vol. 2789, No. 1. – Art. 040124. – P. 1–8. – DOI: 10.1063/5.0145476.

Статья поступила в редакцию: 05.08.2026
Статья принята к публикации: 10.08.2026
Статья опубликована: 28.09.2026

УДК 677.3+546.6

Physicochemical investigation of developed composite dyes for thermal dyeing in the finishing of textile fabrics and fibers

Kasimova Malika
Doctoral student of the State Unitary Enterprise Fan va tarakkiyot Tashkent State Technical University
Republic of Uzbekistan, Tashkent
E-mail: aminbek0486@gmail.com

Negmatova Komila
doctor of Technical Sciences, Senior Researcher
Secretary of the State Unitary Enterprise Fan va tarakkiyot Tashkent State Technical University
Republic of Uzbekistan, Tashkent
E-mail: fan_va_taraqqiyot@mail.ru

Nodira Abed
doctor of Technical Sciences, Professor, Director of the State Institute Fan va Tarakkiyot at the Tashkent State Technical University named after Islam Karimov
Republic of Uzbekistan, Tashkent

Библиографическое описание: Касымова М.Н. кизи, Негматова К.С., Абед Н.С. Исследование физико-химических свойств разработанных композиционных красителей для термического крашения, применяемых при отделке тканей и волокон // Universum: технические науки : электрон. научн. журн. 2026. 9(150). URL: https://7universum.com/ru/tech/archive/item/23295

For citation: Kasimova M., Negmatova K., Nodira A. Physicochemical investigation of developed composite dyes for thermal dyeing in the finishing of textile fabrics and fibers // Universum: Technical Sciences : electronic scientific journal. 2026. No. 9(150). Available at: https://7universum.com/ru/tech/archive/item/23295

Исследование физико-химических свойств разработанных композиционных красителей для термического крашения, применяемых при отделке тканей и волокон

Касымова Малика Носир кизи
докторант
Государственного унитарного предприятия Фан ва тараққиёт, Ташкентский государственный технический университет
Республика Узбекистан, г. Ташкент

Негматова Комила Сайибжановна
д-р техн. наук
ст. науч. сотр Государственного унитарного предприятия Фан ва тараққиёт, Ташкентский государственный технический университет
Республика Узбекистан, г. Ташкент

Абед Нодира Сайибжановна
д-р техн. наук, проф., директор
Государственный институт Фан ва тараққиёт при Ташкентском государственном техническом университете имени Ислама Каримова
Республика Узбекистан, г. Ташкент

Abstract

The article presents extended results of comprehensive studies on the physicochemical regularities of the thermal dyeing process of fabrics based on protein fibers using composite dyes containing salts of polyvalent metals and phenolic derivatives. Particular attention is paid to investigating the influence of the nature of polyvalent metal salts ($Fe_2(SO_4)_3$, $CoCl_2$, $CuSO_4$, $NiCl_2$), as well as process parameters such as temperature and dyeing duration, on the formation of color characteristics, intensity, depth, and fastness of natural silk coloration.

Experimental results have shown that the composition of the dyeing system plays a decisive role in determining the quality of coloration. It has been established that the most effective system is based on iron (III) sulfate and resorcinol, which ensures uniform, rich, and durable colors with high resistance to physicochemical воздействия. It is demonstrated that increasing the dyeing temperature and prolonging the treatment time of the material in the dye solution enhance the diffusion of the dye into the fiber structure, leading to increased color intensity, greater depth of shade, and improved performance properties.

The obtained results have practical significance and can be used in the development of resource-saving and environmentally friendly technologies for dyeing natural silk, as well as other protein-based textile materials, using next-generation composite dyes.

Аннотация

В статье представлены расширенные результаты комплексных исследований физико-химических закономерностей процесса термического крашения тканей на основе белковых волокон с применением композиционных красителей, содержащих соли поливалентных металлов и фенольные производные. Особое внимание уделено изучению влияния природы солей поливалентных металлов ($Fe_2(SO_4)_3$, $CoCl_2$, $CuSO_4$, $NiCl_2$), а также технологических

параметров процесса — температуры и продолжительности крашения — на формирование цветовых характеристик, интенсивность, глубину и устойчивость окраски натурального шелка.

Экспериментальные результаты показали, что состав красильной композиции оказывает решающее влияние на качество окрашивания. Установлено, что наиболее эффективной является система на основе сульфата железа (III) и резорцина, обеспечивающая получение равномерных, насыщенных и устойчивых окрасок с высокими показателями прочности к физико-химическим воздействиям. Показано, что повышение температуры процесса крашения и увеличение времени выдержки материала в красильном растворе способствуют усилению диффузии красителя в структуру волокна, что приводит к увеличению интенсивности окраски, глубины цвета и улучшению эксплуатационных характеристик.

Полученные результаты имеют практическую значимость и могут быть использованы при разработке ресурсосберегающих и экологически безопасных технологий крашения натурального шелка, а также других белковых текстильных материалов с использованием композиционных красителей нового поколения.

Keywords: protein fibers, natural silk, thermal dyeing, composite dyes, polyvalent metal salts, iron(III) sulfate, resorcinol, hydroquinone, color characteristics, color fastness, resource-efficient technology.

Ключевые слова: белковые волокна, натуральный шелк, термическое крашение, композиционные красители, соли поливалентных металлов, сульфат железа (III), резорцин, гидрохинон, цветовые характеристики, прочность окраски, ресурсосберегающая технология.

Introduction

Under conditions of intense market competition, achieving a wide color gamut and high quality of finished textile products is one of the key requirements of the textile industry. During service, textile materials are exposed to various external factors, including washing, abrasion, and sunlight. Therefore, developing an accessible method for preserving the brightness, color saturation, and color fastness of dyed textile materials during their use is of considerable importance [1–3].

The dyeing process includes the diffusion of the dye to the fiber surface, its adsorption onto the surface, diffusion into the fiber structure, and fixation within the fiber. This sequence constitutes the mechanism of dye formation on textile fibers. Insoluble azo dyes are capable of penetrating textile materials through capillary action and diffusion processes, resulting in intensive coloration.

Dyes are synthesized directly within protein-based fibers and fabrics through the coupling of azo and diazo components, represented by naphthol compounds and diazonium salts, respectively. During the dyeing process, protein-based fabrics are impregnated with an alkaline solution of the azo component, dried, and subsequently treated with an aqueous solution of the diazo component at pH 7–9 under cold conditions. In addition, azogen systems, which collectively refer to the azo and diazo components used for the in situ synthesis of water-insoluble azo dyes, are widely employed. This dyeing technique is known as cold (ice) dyeing and consists of treating fabrics impregnated with an alkaline azo-component solution in a cooled diazonium salt solution, followed by squeezing and aging until the azo-coupling reaction is completed.

In this method, the dye is synthesized directly within the fiber from intermediate compounds. Since the resulting dye is insoluble in water, the dyed material exhibits excellent fastness to wet treatments [4].

However, pretreatment with an alkaline azo-component solution makes this method unsuitable for dyeing natural silk. Conventional methods of dyeing natural silk with direct dyes do not provide sufficiently durable dark shades. Natural silk is commonly dyed with reactive dyes in either alkaline or acidic media. Dyeing in alkaline media provides high color fastness but carries the risk of degradation of the protein fibers due to the action of alkaline solutions at elevated temperatures. In acidic media, the dye is fixed to the fiber mainly through ionic and intermolecular interactions rather than covalent bonds, as occurs during alkaline dyeing [5].

Therefore, the most rational approach to the coloration of natural silk is the development of dyeing compositions based on polyvalent metal salts capable of forming colored compounds directly within the fiber structure.

The objective of this study was to investigate the physicochemical properties of newly developed composite dyes for thermal dyeing applied in the finishing of protein-based fabrics.

Materials

The objects of the study included protein fibers and fabrics, polyvalent metal salts, copper sulfate, iron acetate, nickel chloride, cobalt chloride, sodium acetate, sodium nitrite, resorcinol, sulfuric acid, hydrochloric acid, nitric acid, industrial waste products, and selected inorganic and organic ingredients.

Research Methods

Experimental investigations were carried out throughout the study. The physicochemical properties of the components were determined using chemical, refractometric, and titrimetric analytical methods. The technological characteristics were evaluated using standardized methods, instruments, and equipment in accordance with the relevant GOST standards adopted in the CIS countries.

Results and Discussion

Fibroin, the principal protein component of natural silk, contains a limited set of amino acid residues in its polymer chain, consisting primarily of glycine, alanine, serine, and tyrosine. The amino groups of these amino acids possess lone pairs of electrons on the nitrogen atom, enabling the formation of coordination or covalent bonds with metal ions. The presence of primary amino groups in the polymer substrate also allows diazotization to produce highly reactive diazonium salts. The coupling of diazonium salts with phenols or aromatic amines results in the formation of colored compounds [6–7].

The study investigated the influence of various polyvalent metal salts on the coloration of natural silk organza fabric. The introduction of alkaline earth, transition, and rare-earth metal cations into the dyeing process significantly increased dye uptake, color intensity, color fastness, and the tensile strength of the silk fibers [8-10].

Table 1 presents the color shades obtained for dyed protein-based fabrics using different polyvalent metal salts.

Table 1.

Color shades obtained for dyed protein-based fabrics

Dyed samples	Polyvalent metal salts
	$Fe_2(SO_4)_3$ (resorcinol)
	$Fe_2(SO_4)_3$ (Dyeing with a daily solution, resorcinol)
	$Fe_2(SO_4)_3$ (pyrocatechin)
	$CoCl_2$ (resorcinol)
	$CuSO_4$ (resorcinol)
	$NiCl_2$ (resorcinol)

The experimental investigations were carried out in several stages:

1. Evaluation of the dyeability of the selected fabric using polyvalent metal salts in combination with resorcinol and hydroquinone.

2. Investigation of the hue and color intensity obtained with different polyvalent metal salts.

3. Study of the effect of dyeing temperature on the color intensity of the fabrics.

4. Evaluation of the possibility of obtaining stable coloration on natural silk under resource-efficient processing conditions using polyvalent metal salts.

To investigate changes in the color intensity of natural silk materials, the following polyvalent metal salts were selected: $Fe_2(SO_4)_3$, $CoCl_2$, $CuSO_4$, and $NiCl_2$, with the aim of identifying the most effective and colorfast dyeing system. Laboratory experiments were performed using organza, a thin, matte, stiff, and transparent fabric made of natural silk, as the model substrate.

The dyeing process was carried out under laboratory conditions. The initial dyeing temperature was 40°C in a solution containing a polyvalent metal salt and the dihydric phenol resorcinol (1,3-dihydroxybenzene, *m*-dihydroxybenzene). The temperature was gradually increased to enhance dye diffusion into the fiber structure [9-10].

The maximum dyeing temperature was 90°C, and the samples were maintained at this temperature for 60 min. In experiments involving iron(III) sulfate, parallel studies were also performed using hydroquinone as a reaction accelerator. In this case, the dyeing solution was aged for 24 h at room temperature before use.

The results presented in Table 1 demonstrate the coloration of natural silk organza using different polyvalent metal salts. The range of colors obtained depends primarily on the nature of the metal ion. As shown by the first entries in Table 1, dyeing with $Fe_2(SO_4)_3$ in the presence of resorcinol produced different color intensities despite identical dyeing times. Organza dyed for 60 min in a freshly prepared solution exhibited lower color intensity than samples dyed in a solution aged for 24 h. Furthermore, the dyeing composition prepared from $Fe_2(SO_4)_3$ and hydroquinone resulted in a pronounced change in the color palette accompanied by a decrease in color intensity.

Based on these results, the iron(III) sulfate–resorcinol system was selected for further investigation as the most effective dye-fixing composition. The subsequent stage of the study focused on evaluating the effect of dyeing time on the intensity of the resulting coloration.

Table 2.

Color shades obtained for dyed protein-based fabrics

Dyed samples	Polyvalent metal salts
	$Fe_2(SO_4)_3$ (resorcinol), 90°C, 3 min
	$Fe_2(SO_4)_3$ (resorcinol), 90°C, 5 min
	$Fe_2(SO_4)_3$ (resorcinol), 90°C, 7 min
	$Fe_2(SO_4)_3$ (resorcinol), 90°C, 10 min
	$Fe_2(SO_4)_3$ (resorcinol), 90°C, 30 min

At this stage of the study, dyeing was carried out under the same temperature conditions (initial temperature 40°C and maximum temperature 90°C), while the fabric holding time was varied at six intervals ranging from 3 to 50 min.

The results presented in Table 2 indicate that a dyeing time of 7 min is sufficient to obtain a color shade comparable to that achieved after 60 min of dyeing. By varying the dyeing time of natural silk in a solution containing a single polyvalent metal salt, it was possible to obtain a wide range of color shades. As the dyeing time decreased, the dyed fabrics exhibited progressively lighter yellowish-brown tones accompanied by a reduction in color depth and intensity.

In the next stage of the study, changes in color intensity were investigated by dyeing the samples in a boiling dye solution based on iron(III) sulfate, while varying the holding time from 3 to 50 min.

Table 3.

Color shades obtained for protein-based fabrics dyed with composite dye formulations

Painted samples	Painting conditions
	$Fe_2(SO_4)_3$ (resorcinol), 90 °C, 3 min
	$Fe_2(SO_4)_3$ (resorcinol), 90 °C, 3 min
	$Fe_2(SO_4)_3$ (resorcinol), 90 °C, 3 min
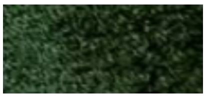	$Fe_2(SO_4)_3$ (resorcinol), 90 °C, 3 min
	$Fe_2(SO_4)_3$ (resorcinol), 90 °C, 3 min
	$Fe_2(SO_4)_3$ (resorcinol), 90 °C, 3 min

Table 3 presents the results of dyeing carried out without preliminary heating. Under these conditions, the dyed fabrics exhibited brighter colors with lighter shades than those obtained by gradual heating, where the dyeing temperature was increased from 40°C to 90°C. As the holding time of the fabric in the dye bath decreased, the color gradually changed from deep, saturated dark shades to lighter and brighter tones. The samples dyed for 50, 30, and 10 min showed no pronounced differences in color intensity; however, they differed in shade depth from the other samples. A sharp decrease in color depth was observed when the dyeing time was reduced to 7 min. With a further reduction in dyeing time, the fabrics developed more muted, earthy color tones.

The dyeing duration also had a significant effect on the hue of the samples. As the dyeing time decreased, reddish shades gradually appeared, while the deep green coloration progressively shifted toward reddish tones.

The subsequent stage of the investigation focused on evaluating the influence of dyeing temperature on the color characteristics of the samples while maintaining a constant dyeing time.

The experiments were performed using the selected iron(III) sulfate system under two different temperature regimes: (I) gradual heating from 40°C to 60°C and higher over a period of 10 min, and (II) dyeing in a preheated solution maintained at 60°C and above for 10 min. It should be noted that resorcinol was used as the fixing component in all experiments.

Table 4.

Color shades obtained for protein-based fabrics dyed with composite dye formulations

Dyed fabric samples	Dyeing conditions	Dyed fabric samples	Dyeing conditions
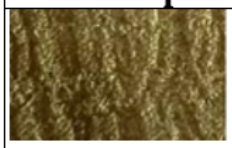	$Fe_2(SO_4)_3$ (rezortsin) 60°C 10 min 40°C	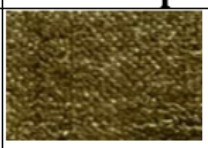	$Fe_2(SO_4)_3$ (rezortsin) 60°C 10 min
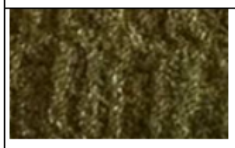	$Fe_2(SO_4)_3$ (rezortsin) 70°C 10 min 40°C		$Fe_2(SO_4)_3$ (rezortsin) 70°C 10 min
	$Fe_2(SO_4)_3$ (rezortsin) 80°C 10 min 40°C		$Fe_2(SO_4)_3$ (rezortsin) 80°C 10 min

Comparison of the dyeing results obtained by gradually increasing the temperature from 40°C to 60°C over 10 min with those obtained under identical conditions at the maximum temperature of 90°C revealed a pronounced color transition from deep, saturated dark green to lighter golden shades. Furthermore, dyeing under continuous temperature increase resulted in enhanced color intensity and greater shade depth.

Based on the results presented in Table 4, it can be concluded that the temperature gradient has a significant influence on the dyeing process. The increase in dyeing temperature, together with continuous heating, promotes higher color intensity and deeper shades in the dyed samples. Stepwise temperature elevation produced brighter and lighter colors with a characteristic luster over the entire temperature range, whereas higher dyeing temperatures resulted in considerably greater color depth and saturation. The possibility of obtaining stable coloration at the minimum temperature of 40°C was also investigated.

Additional experiments were carried out under constant-temperature conditions (40°C) while varying the holding time in the dye bath from 10 to 60 min. The objective of this stage was to evaluate the feasibility of dyeing at the minimum temperature and to investigate the effect of dyeing time on color development under these conditions. The corresponding results are presented in Table 5.

Table 5.

Color shades obtained for protein-based fabrics dyed with composite dye formulations

Dyed fabric samples	Dyeing conditions
	$Fe_2(SO_4)_3$ (rezortsin) ⇩ 40°C 10 min
	$Fe_2(SO_4)_3$ (rezortsin) ⇩ 40°C 20 min
	$Fe_2(SO_4)_3$ (rezortsin) ⇩ 40°C 30 min
	$Fe_2(SO_4)_3$ (rezortsin) ⇩ 40°C 40 min
	$Fe_2(SO_4)_3$ (rezortsin) ⇩ 40°C 50 min

The results presented in Table 5 confirm the existence of a minimum effective dyeing temperature for natural silk treated with a resorcinol solution containing polyvalent metal salts, which is sufficient to produce dark, highly intense colors with considerable shade depth. These findings also demonstrate the feasibility of dyeing natural silk fibers while maintaining high color intensity and shade depth even under relatively low-temperature conditions.

Conclusion

The study established that the principal factors influencing the shade depth of dyed fabrics are the dyeing temperature and the holding time of the material in the dye bath. The use of polyvalent metal salt solutions at elevated temperatures makes it possible to obtain and maintain bright, saturated, and durable colors on dyed textile materials.

The duration of the dyeing process also has a significant effect on color brightness and saturation. As shown in Table 5, both parameters increase progressively with increasing holding time of the fabric in the dye bath, resulting in deeper and more intense coloration.

References

1. Sadovsky V.V., Nesmelov N.M. [Commodity science and examination of textile products]. – Minsk: Belarus State Economic University, 2012. – 526 P. (In Russ.)

2. Sklyannikov V.P. [Consumer properties of textile products]. – Moscow: Ekonomika, 1982. – 160 P. (In Russ.)
3. Pichkhadze Sh.V., Soshina S.M. [Weighting and finishing of natural silk fabrics]. – Moscow: [s. n.], 1990. – 56 P. (In Russ.)
4. Davlatov R.M., Ismailov R.I. [Modification of protein fibers]: monograph. – Tashkent: Navruz Publishing House, 2016. – 160 P. (In Russ.)
5. Babakhanova M.A., Raupova D.N., Dzhabarov B.T., Bozorov A.N. Study of some properties of composite paints and varnishes used in the leather, footwear and other industries // Universum: Technical Sciences. – 2025. – Vol. 5, No. 11 (140). – P. 13–16. (In Russ.)
6. Negmatov S.S., Abed N.S., Sherkulova N.R., Davlatov R.M. [Polymer compositions reducing the influence of physicomechanical factors on protein fibers during primary processing] // Kompozitsion Materiallar: Scientific-Technical and Practical Journal. – 2020. – No. 4. – P. 55–60. (In Russ.)
7. Abdurakhmonova Sh.G., Majidova Sh.G., Rakhimova Z.M., Abduqodirova N.M., Abdurakhmonov U., Ismailov I.I. [Dyeing compositions as promising substitutes for synthetic dyes] // Proceedings of the Republican Scientific and Technical Conference «New Technologies for Obtaining Composite Materials Based on Local Raw Materials and Their Application in Production». – 2005. – P. 131–132. (In Russ.)
8. Abdurakhmonova Sh.G., Rakhimova Z.M., Abduqadirova N.M., Ganiev A.V., Turdialiev S.M., Ismailov I.I. [Dyeing compositions based on polyvalent metals for dyeing wool fibers] // Proceedings of the Republican Scientific and Technical Conference «New Technologies for Obtaining Composite Materials Based on Local Raw Materials and Their Application in Production». – 2005. (In Russ.)
9. Negmatov S.S., Babakhanova M.A., Ikramova M.E., Raupova D.N., Dzhabarov B.T., Shamsieva S.S., Bozorov A.N. Development of effective compositions of composite paints and varnishes for use in the leather and footwear industry and a comparative study of their physicochemical and performance properties // Universum: Technical Sciences. – 2026. – Vol. 3, No. 3 (144). – P. 39–45. (In Russ.)
10. Davlatov R.M. [Sorption capacity of modified silk during dyeing] // Proceedings of the Conference «Current Problems of Physics and Chemistry of Polymer Composites and Technology of Structural Materials». – 2017. (In Russ.)

Статья поступила в редакцию: 19.08.2026
Статья принята к публикации: 28.08.2026
Статья опубликована: 28.09.2026

УДК 628.3+677

Application of modified cellulose acetate composite filters for the removal of pollutants from textile industry wastewater

Sultanov Sanjar
doctor of Chemical Sciences (DSc)
Senior Researcher, Head of the Laboratory of the State Institution Fan va Taraqqiyot under Tashkent State Technical University
Republic of Uzbekistan, Tashkent
E-mail: fan_va_taraqqiyot@mail.ru

Anvarova Zarina
Doctoral Student
at the State Institution Fan va Taraqqiyot under Tashkent State Technical University
Republic of Uzbekistan, Tashkent

Применение модифицированных композиционных фильтров на основе ацетатцеллюлозы для очистки сточных вод текстильной промышленности от загрязняющих веществ

Султанов Санжар Уразалиевич
д-р хим. наук (DSc), ст. науч. сотр., заведующий лабораторией Государственного учреждения Фан ва тараккиёт при Ташкентском государственном техническом университете
Республика Узбекистан, г. Ташкент

Анварова Зарина Анвар кизи
докторант
Государственного учреждения Фан ва тараққиёт при Ташкентском государственном техническом университете
Республика Узбекистан, г. Ташкент

Abstract

This article investigates the potential of modified cellulose acetate-based composite filter materials for the effective removal of dyes, colloidal substances, and organic pollutants from textile industry wastewater. Composite filter materials based on diacetylcellulose were prepared using various organo-inorganic components, including titanium dioxide, silicon dioxide, activated carbon, and chitosan. The effects of the type, concentration, and ratio of modifiers on the porosity, water

Библиографическое описание: Султанов С.У., Анварова З.А. кизи Применение модифицированных композиционных фильтров на основе ацетатцеллюлозы для очистки сточных вод текстильной промышленности от загрязняющих веществ // Universum: технические науки : электрон. научн. журн. 2026. 9(150). URL: https://7universum.com/ru/tech/archive/item/23356

For citation: Sultanov S., Anvarova Z. Application of modified cellulose acetate composite filters for the removal of pollutants from textile industry wastewater // Universum: Technical Sciences : electronic scientific journal. 2026. No. 9(150). Available at: https://7universum.com/ru/tech/archive/item/23356

permeability, sorption capacity, and mechanical strength of the filter materials were studied. Structural and morphological analyses demonstrated that the formation of a homogeneous porous structure in the composite materials enhances the efficiency of filtration and sorption processes. Based on the experimental results, an optimal composition containing diacetylcellulose, plasticizer, fillers, TiO_2, activated carbon, and chitosan was proposed. The obtained filter materials were tested in dye baths, confirming their high adsorption properties, mechanical stability, and potential for long-term operation. The optimal porosity was found to be within the range of 60–70 %, providing a favorable balance between purification efficiency and filtration rate. The developed composite filter materials were evaluated as promising materials for textile wastewater treatment, water reuse, and reduction of environmental pollution. The relationship between composition–structure–property was identified as a key factor governing the sorption and filtration characteristics of the materials. The obtained results demonstrate the potential application of modified cellulose acetate-based filters in industrial enterprises to reduce wastewater color and organic pollution, improve the economic efficiency of treatment processes, and contribute to reducing water scarcity.

Аннотация

В статье исследована возможность применения модифицированных композиционных фильтрующих материалов на основе ацетатцеллюлозы для эффективного удаления красителей, коллоидных и органических загрязняющих веществ из сточных вод текстильной промышленности. На основе диацетатцеллюлозы получены композиционные фильтрующие материалы с использованием различных органо-неорганических компонентов, включая диоксид титана, диоксид кремния, активированный уголь и хитозан. Изучено влияние вида, содержания и соотношения модифицирующих компонентов на пористость, водопроницаемость, сорбционную способность и механическую прочность фильтрующих материалов. Результаты структурных и морфологических исследований показали, что формирование однородной пористой структуры композиционных материалов способствует повышению эффективности процессов фильтрации и сорбции. На основании полученных экспериментальных результатов предложен оптимальный состав композиционного материала, включающий диацетатцеллюлозу, пластификатор, наполнители, TiO_2, активированный уголь и хитозан. Полученные фильтрующие материалы испытаны в условиях красильных ванн, что подтвердило их высокие адсорбционные свойства, механическую стабильность и возможность длительной эксплуатации. Оптимальная пористость материалов составила 60–70 %, при которой обеспечивается рациональный баланс между эффективностью очистки и скоростью фильтрации. Разработанные композиционные фильтрующие материалы могут рассматриваться как перспективные материалы для очистки сточных вод текстильной промышленности, повторного использования воды и снижения экологической нагрузки. Установлена взаимосвязь «состав–структура–свойство», определяющая сорбционные и фильтрационные характеристики материалов. Полученные результаты свидетельствуют о перспективности применения модифицированных ацетатцеллюлозных фильтров на промышленных предприятиях

Keywords: cellulose acetate, composite filter material, textile industry, wastewater, water purification, modification, activated carbon, chitosan, titanium dioxide, silicon dioxide, sorption, adsorption, porosity, filtration, purification efficiency.

Ключевые слова: ацетатцеллюлоза, композиционный фильтрующий материал, текстильная промышленность, сточные воды, очистка воды, модификация, активированный уголь, хитозан, диоксид титана, диоксид кремния, сорбция, адсорбция, пористость, фильтрация, эффективность очистки.

Introduction

Today, along with the rapid development of the textile industry, the effective treatment and reuse of wastewater generated during production processes is one of the important environmental challenges. Textile enterprises consume large amounts of water during dyeing, washing, bleaching, and finishing processes, resulting in the formation of wastewater containing dyes, organic compounds, salts, and other pollutants [3; 4; 7].

Various methods, including coagulation-flocculation, adsorption, oxidation, flotation, and membrane filtration, are widely used for textile wastewater treatment. However, due to the complex composition of wastewater and the presence of different types of pollutants, the use of a single treatment method does not always provide the required purification efficiency [3;7]. In particular, adsorption and membrane filtration are considered promising approaches for the removal of dye compounds from wastewater [4–6].

During the adsorption process, activated carbon, silicon dioxide, zeolites, and various carbon-based materials are widely used as effective adsorbents. These materials can remove dye molecules due to their porous structure and developed specific surface area [4; 6]. Membrane technologies make it possible to separate suspended particles and dissolved components based on membrane pore size and selective permeability. However, membrane fouling, service life, and operating costs remain important limitations in the application of these technologies [1; 5].

From this perspective, the use of cellulose acetate as a polymer matrix is considered a promising approach. Modification of cellulose acetate-based filter and membrane materials with various modifiers makes it possible to control their porosity, water permeability, mechanical strength, and sorption properties. Recent studies have demonstrated the potential of cellulose acetate-based fibrous and nanofibrous materials for the removal of dyes, including methylene blue, from aqueous media [2].

At the same time, incorporation of organic and inorganic components such as TiO_2, SiO_2, activated carbon, and chitosan into a cellulose acetate matrix can improve the functional properties of composite materials. Such components play an important role in increasing the number of adsorption sites, developing the porous structure, and improving the mechanical stability of filter materials [4; 2; 8].

The aim of this study is to evaluate the applicability of modified cellulose acetate-based composite filter materials for the effective removal of dyes, colloidal substances, and organic pollutants from textile industry wastewater.

The study focuses on determining the filtration and sorption properties of modified cellulose acetate composite filters, evaluating their wastewater treatment efficiency, determining the optimal porosity of the filter material, and assessing their applicability under dye-bath conditions. Based on the experimental results, the optimal composition and practical potential of the developed composite filters for textile wastewater treatment were evaluated.

Materials

The materials used in this study included diacetylcellulose as the polymer matrix, titanium dioxide (TiO_2), silicon dioxide (SiO_2), chitosan, activated carbon, and plasticizer as the main modifying components. Textile industry wastewater and dye-bath wastewater were used as the objects of the study. The selected organic and inorganic components were used to prepare modified cellulose acetate-based composite filter materials with controlled porous structures and improved sorption and filtration properties.

Research Methods

Experimental investigations were carried out throughout the study. The composition, physicochemical, structural, and filtration properties of the developed modified cellulose acetate-based composite filter materials were investigated using appropriate analytical methods. Fourier-transform infrared (FTIR) spectroscopy was used to identify the functional groups and chemical interactions between the components. Scanning electron microscopy (SEM) was employed to examine the surface morphology and porous structure of the composite filter materials. The porosity, water permeability, water absorption, swelling, and mechanical strength of the obtained materials were determined using standardized experimental procedures. The purification efficiency of the composite filters was evaluated using textile industry wastewater and dye-bath wastewater. The changes in the main wastewater quality parameters before and after filtration were analyzed to determine the effectiveness of the developed filter materials. The experimental data were processed using mathematical and statistical methods to determine the optimal composition and operating characteristics of the composite filter materials.

Results and Discussion

Several types of cellulose acetate were selected as binders for the preparation of composite filter materials. Cellulose acetate is characterized by good film-forming ability, chemical stability, and mechanical properties. It is readily soluble in organic solvents such as acetone, ethanol, and methylene chloride.

To improve the porosity, mechanical strength, and sorption properties of the cellulose acetate-based filter materials, SiO_2, TiO_2, activated carbon, and chitosan were incorporated into the composition. SiO_2 contributes to structural stabilization and the formation of a stable porous structure**.** TiO_2 contributes to the functional properties and structural modification of the material. Activated carbon, due to its high sorption capacity, contributes to the removal of organic compounds and dyes from wastewater, while chitosan enhances the sorption properties through its functional amino groups.

The composite filter materials were prepared under laboratory conditions. Cellulose acetate was dissolved in an organic solvent and stirred continuously at 40–50 °C to obtain a homogeneous solution. The solution was then maintained under vacuum for 20–30 min to remove entrapped air bubbles. Polyethylene glycol (PEG) was added at a concentration of 5 wt.% as a plasticizing and pore-forming component. The pre-prepared SiO_2, TiO_2, activated carbon, and chitosan were then introduced in predetermined amounts and mixed uniformly for 10–15 min.

The resulting composite mixture was poured into molds and dried at 25–60 °C by evaporating the solvent to obtain film-like filter materials. The developed materials exhibited high porosity, good mechanical strength, and enhanced sorption properties.

The incorporation of the selected fillers improved the water permeability, sorption characteristics, and operational stability of the materials. Based on the experimental results, optimal compositions of the composite filter materials for textile wastewater treatment were selected.

The optimal compositions of the developed composite filter materials for textile wastewater treatment are presented in Table 1.

Table 1.

Optimal composition of the developed composite filter materials for textile wastewater treatment

Components	**Composition of components, wt.%**		
	CFM- 1	**CFM -2**	**CFM -3**
Diacetylcellulose	100	100	100
Polyethylene glycol (PEG)	5	5	5
Titanium dioxide (TiO_2)	8-	6	4
Silicon dioxide (SiO_2)	10	8	6
Chitosan	8	6	4
Activated carbon	10	10	10

To determine the chemical structure of the composite filter material and the effect of the fillers incorporated into its composition, Fourier-transform infrared spectroscopy (FTIR) analysis was performed **(**Fig. 1**).**

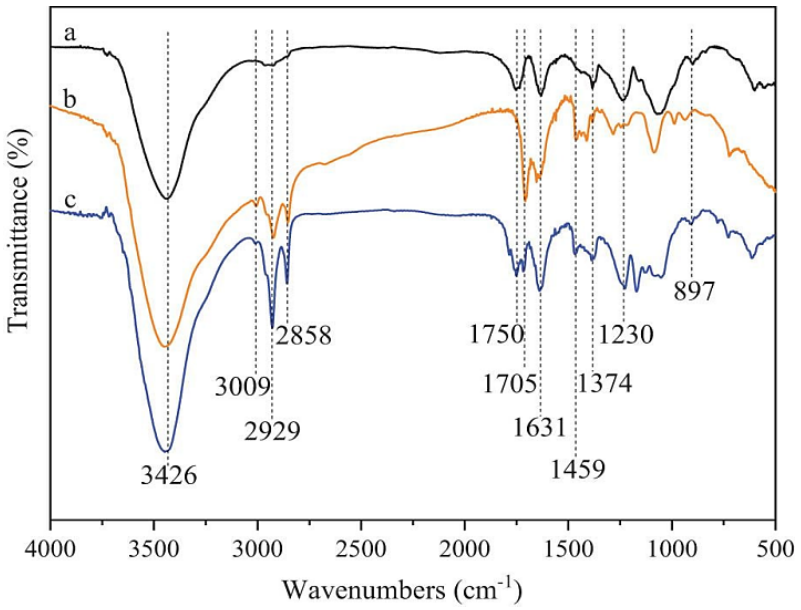

Figure 1. FTIR spectra of cellulose acetate-based composite materials filled with activated carbon, chitosan, TiO_2, and SiO_2

The analysis of the spectra showed that the broad absorption band observed in the range of 3200–3500 cm^{-1} corresponds to hydroxyl (–OH) groups and is associated with the hydroxyl groups present in cellulose acetate and SiO_2. At the same time, the broadening and increase in intensity of the band in this region indicate the formation of hydrogen bonds between the components. The absorption bands observed at around 1600–1650 cm^{-1} are attributed to amino ($–NH_2$) groups of chitosan, confirming the presence of the biopolymer in the composite material. The band in the range of 1730–1750 cm^{-1} corresponds to carbonyl (C=O) groups characteristic of cellulose acetate and indicates that the main polymer matrix is retained in the composite. The strong absorption bands observed in the 1000–1200 cm^{-1} region are attributed to silicon–oxygen (Si–O–Si) bonds, confirming the presence of the SiO_2 filler. The bands in the 700–900 cm^{-1} range are attributed to titanium–oxygen (Ti–O) bonds, indicating the incorporation of TiO_2 nanoparticles into the composite. In addition, absorption bands corresponding to aromatic C=C bonds were observed in the 1500–1600 cm^{-1} region, which can be associated with the presence of activated carbon.

The FTIR spectral analysis results fully confirmed the presence of cellulose acetate, chitosan, SiO_2, TiO_2, and activated carbon in the composite material. The shifts of the absorption bands and changes in their intensity indicate the occurrence of interactions between the components, including hydrogen bonding and physical interactions. This indicates the formation of a stable structure in the composite material.

To investigate the surface morphology of the composite materials, scanning electron microscopy (SEM) analysis was performed (Fig. 2). According to the obtained results, the pure cellulose acetate sample exhibited a relatively smooth and homogeneous surface. A low number of pores and a densely packed structure were observed.

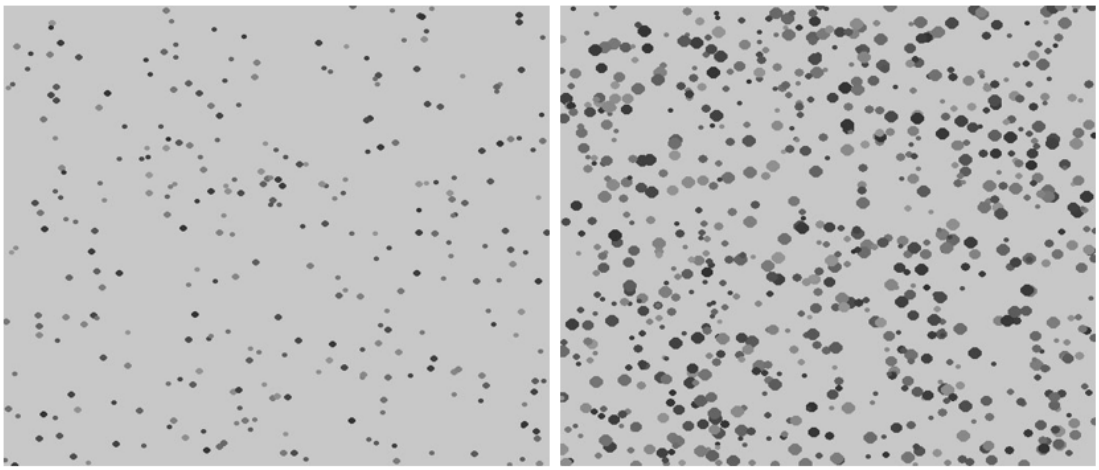

Figure 2. SEM images of cellulose acetate-based materials: (a) pure cellulose acetate; (b) cellulose acetate composite material containing activated carbon, chitosan, TiO_2, and SiO_2

SEM analysis revealed clear differences in the surface morphology of pure and modified cellulose acetate materials. The pure cellulose acetate sample (Fig. 2a) exhibited a relatively smooth and homogeneous surface with a dense structure and a low number of visible pores. After incorporation of activated carbon, chitosan, TiO_2, and SiO_2, the surface morphology changed considerably (Fig. 2b), showing a rougher and more porous structure with an increased number and size of pores. The inorganic particles were relatively uniformly distributed throughout the polymer matrix, while the incorporation of chitosan contributed to the formation of additional active sites on the surface. These morphological changes are favorable for improving the sorption and filtration properties of the composite material.

The efficiency of cellulose acetate-based composite filter materials is largely determined by their porous structure and permeability. Porosity directly affects the ability of the material to transport liquids and gases and is closely related to the internal structure, filler distribution, and interactions between the components.

In this study, the porosity and permeability of filter materials based on different types of cellulose acetate were comparatively investigated. The total porosity was determined using the pycnometric method based on the actual and theoretical densities of the materials in accordance with GOST 28513-90. The permeability characteristics were evaluated by determining the volume of liquid or gas passing through the filter material per unit of time under a specified pressure.

The results obtained for filter materials based on monoacetate, diacetate, and triacetate cellulose demonstrated that the type of cellulose acetate significantly affects the structural and filtration properties of the materials. Among the investigated samples, the diacetate cellulose-based material exhibited the most favorable combination of porosity and permeability, indicating a more suitable porous structure for filtration applications. In contrast, triacetate cellulose showed comparatively lower permeability, which was associated with its denser structure and lower porosity. Based on these results, diacetate cellulose was selected as the optimal polymer matrix for the subsequent preparation of modified composite filter materials.

Table 2.

Porosity and filtration properties of cellulose acetate-based filter materials

№	Material properties	Monoacetate cellulose	Diacetate cellulose	Triacetate cellulose	Determination method
1	Porosity, %	38 ± 1.2	45 ± 1.4	30 ± 1.0	GOST 18898-89
2	Permeability, cm³/s	0.70 ± 0.03	0.90 ± 0.04	0.60 ± 0.03	GOST 3584-73
3	Density, g/cm³	1.18 ± 0.02	1.20 ± 0.02	1.28 ± 0.03	GOST 28513-90
4	Water absorption, %	20 ± 0.8	18 ± 0.7	12 ± 0.6	Gravimetric method
5	Average pore diameter, μm	10 ± 0.5	14 ± 0.7	8 ± 0.4	Microscopic analysis
6	Filtration efficiency, %	82 ± 1.5	88 ± 1.3	80 ± 1.6	Experimental method

Values are presented as mean ± standard deviation (SD), n = 3.

The main practical performance of the developed composite filter materials was evaluated based on their ability to reduce the major pollutants present in textile wastewater. Particular attention was paid to color intensity, chemical oxygen demand (COD), biochemical oxygen demand (BOD), and suspended solids, as these parameters are important indicators of wastewater quality.

Textile wastewater was treated using the developed CFM-1, CFM-2, and CFM-3 composite filters. The changes in the main wastewater quality parameters before and after filtration were compared. The results obtained for the three filter compositions are presented in Table 3.

Table 3.

Changes in the main quality parameters of textile wastewater after filtration

Parameter	Before treatment	CFM-1	CFM-2	CFM-3
Color intensity, %	100 ± 1.0	18 ± 0.8	12 ± 0.6	15 ± 0.7
COD, mg/L	620 ± 12	145 ± 5	105 ± 4	125 ± 5
BOD, mg/L	210 ± 6	52 ± 3	38 ± 2	45 ± 3
Suspended solids, mg/L	185 ± 5	32 ± 2	24 ± 1	28 ± 2

Values are presented as mean ± standard deviation (SD), n = 3.

The results presented in Table 3 indicate that all developed composite filter materials substantially reduced the main pollution parameters of textile wastewater. The most pronounced purification effect was observed for CFM-2, which reduced color intensity from 100 % to approximately 12 %, COD from 620 to 105 mg/L, BOD from 210 to 38 mg/L, and suspended solids from 185 to 24 mg/L.

The higher efficiency of CFM-2 can be associated with the balanced ratio of the modifying components in its composition. The combination of activated carbon, SiO_2, TiO_2, and chitosan provides favorable conditions for the retention of dye molecules, suspended particles, and organic pollutants. CFM-1 and CFM-3 also demonstrated significant purification efficiency, although their overall performance was somewhat lower than that of CFM-2.

Thus, the comparative results suggest that CFM-2 represents the most promising composition for the treatment of textile wastewater, providing a favorable combination of filtration and sorption properties. The developed composite filter materials can therefore be considered promising for further practical application in textile wastewater treatment.

Conclusion

The results of this study demonstrate the potential of modified cellulose acetate-based composite filter materials for the treatment of textile industry wastewater. Among the investigated cellulose acetate types, diacetate cellulose showed the most favorable filtration characteristics, with a porosity of 45 %, permeability of 0.90 cm^3/s, and filtration efficiency of 88 %, and was therefore selected as the polymer matrix.

The incorporation of SiO_2, TiO_2, activated carbon, and chitosan into the cellulose acetate matrix improved the functional properties of the developed composite filters. Comparative evaluation of CFM-1, CFM-2, and CFM-3 showed that the composition and ratio of the modifying components significantly affected the filtration performance.

Among the developed materials, CFM-2 demonstrated the most favorable overall purification performance, showing a greater reduction in color intensity, COD, BOD, and suspended solids compared with the other compositions. This effect can be attributed to the balanced composition of the polymer matrix and functional fillers, which provides favorable filtration and sorption properties.

Overall, the developed modified cellulose acetate-based composite filters, particularly CFM-2, demonstrate considerable potential for textile wastewater treatment and may serve as a basis for further optimization and practical application.

References

1. Electrospinning of cellulose acetate for methylene blue dye removal. Hybrid Advances. – 100205 // Hybrid Advances. – 2024. – Vol. 6.
2. Environmental Impacts and Biological Technologies Toward Sustainable Treatment of Textile Dyeing Wastewater: A Review // Sustainability. – 2024. – Vol. 16, No. 24.
3. Fernandes A. et al. Textile Wastewater Treatment by Membrane and Electrooxidation Processes: A Critical Review // Clean Technologies. – 2026. – Vol. 8. – DOI: 10.3390/cleantech8010009.
4. Recent Strategies for the Remediation of Textile Dyes from Wastewater: A Systematic Review // Toxics. – 2023. – Vol. 11.
5. Remediation of textile effluents by membrane based treatment techniques: A state of the art review // Journal of Environmental Management. – 2015. – Vol. 147. – DOI: 10.1016/j.jenvman. 2014.08.008.
6. Review of activated carbon adsorbent material for textile dyes removal: Preparation, and modeling // Current Research in Green and Sustainable Chemistry. – 2022. – Vol. 5. – DOI: 10.1016/j.crgsc.2022.100325.
7. Samsami S., Mohamadizaniani M., Sarrafzadeh M.H., Rene E.R., Firoozbahr M. Recent advances in the treatment of dye-containing wastewater from textile industries: Overview and perspectives. Process Safety and Environmental Protection. – 2020. – Vol. 143. – P. 138–163. DOI: 10.1016/j.psep.2020.05.034.
8. Towards advanced aqueous dye removal processes: A short review on the versatile role of activated carbon // Journal of Environmental Management. – 2012. – Vol. 102. – DOI: 10.1016/ j.jenvman.2012.02.021.

INFRASTRUCTURE AND TRANSPORT

CONSTRUCTION, ARCHITECTURE AND HOUSING AND UTILITIES

Статья поступила в редакцию: 25.08.2026
Статья принята к публикации: 04.09.2026
Статья опубликована: 28.09.2026

УДК 666.3+553.6

DOI: 10.32743/UniTech.2026.150.9.23374

Determining the optimal bentonite content for ceramic brick production

Razzakov Sobirjon
Doctor of Technical Sciences, Professor
Namangan State Technical University,
Republic of Uzbekistan, Namangan

Qayumov Dilshod
senior Lecturer
Namangan State Technical University
Republic of Uzbekistan, Namangan
E-mail: sobirjonrsj@gmail.com

Martazaev Abdurasul
Associate Professor
Namangan State Technical University
Republic of Uzbekistan, Namangan
E-mail: dil_ko91@mail.ru

Библиографическое описание: Раззаков С., Каюмов Д., Мартазаев А. Определение оптимального содержания бентонита в составе керамического кирпича // Universum: технические науки : электрон. научн. журн. 2026. 9(150). URL: https://7universum.com/ru/tech/archive/item/23374

For citation: Razzakov S., Qayumov D., Martazaev A. Determining the optimal bentonite content for ceramic brick production // Universum: Technical Sciences : electronic scientific journal. 2026. No. 9(150). Available at: https://7universum.com/ru/tech/archive/item/23374

Определение оптимального содержания бентонита в составе керамического кирпича

Раззаков Собиржон
д-р техн. наук, проф.
Наманганский государственный технический университет
Республика Узбекистан, г. Наманган

Каюмов Дилшод
ст. преп
Наманганский государственный технический университет
Республика Узбекистан, г. Наманган

Мартазаев Абдурасул
д-р филос. по техн. наукам (PhD), доц.
Наманганский государственный технический университет
Республика Узбекистан, г. Наманган

Abstract

The study investigates the effect of bentonite clay addition on the compressive strength of ceramic bricks produced from locally available clay raw materials. Bentonite was incorporated into the ceramic mixture at contents ranging from 3 to 30 % with an increment of 3 %. Experimental brick specimens were prepared and tested to evaluate the influence of bentonite content on their compressive strength. The results demonstrated that the addition of bentonite up to 12 % significantly improved the strength characteristics of the ceramic bricks. At a bentonite content of 12 %, the compressive strength reached 84.0 kg/cm², compared with 67.2 kg/cm² for the control specimen, corresponding to an increase of approximately 25 %. Further increasing the bentonite content resulted in a gradual reduction in compressive strength. At 30 % bentonite, the compressive strength decreased to 58.2 kg/cm², which was 13.4 % lower than the control value. The observed increase in strength at moderate bentonite contents can be attributed to the fine and highly dispersed structure of bentonite, which contributes to filling interparticle voids and improving the density of the ceramic mass during firing. At higher contents, increased water absorption, drying shrinkage, and the formation of internal microcracks may adversely affect the mechanical properties. Based on the experimental results, 12 % bentonite was identified as the optimal content. The findings demonstrate the potential of bentonite as an effective mineral additive for improving the compressive strength and optimizing the composition of ceramic bricks produced from locally available clay raw materials.

Аннотация

В статье исследовано влияние добавки бентонитовой глины на прочность при сжатии керамического кирпича, изготовленного на основе местного глинистого сырья. Бентонит вводился в состав керамической массы в количестве от 3 до 30 % с шагом 3 %. Были изготовлены и испытаны экспериментальные образцы кирпича для оценки влияния содержания бентонита на их прочность при сжатии. Результаты исследований показали, что увеличение содержания бентонита до 12 % способствует значительному повышению прочностных характеристик керамического кирпича. При содержании бентонита 12 % прочность при сжатии достигла 84,0 кг/см² по сравнению с 67,2 кг/см² у контрольного

образца, что соответствует увеличению примерно на 25 %. Дальнейшее повышение содержания бентонита приводило к постепенному снижению прочности. При содержании бентонита 30 % прочность при сжатии снизилась до 58,2 кг/см², что на 13,4 % ниже контрольного значения. Повышение прочности при умеренном содержании бентонита может быть связано с его тонкодисперсной структурой, способствующей заполнению межчастичных пустот и уплотнению керамической массы в процессе обжига. При повышенном содержании бентонита увеличение водопотребности, усадка при сушке и образование внутренних микротрещин могут отрицательно влиять на механические свойства кирпича. На основании экспериментальных результатов оптимальным содержанием бентонита определено 12 %. Полученные результаты подтверждают перспективность применения бентонита в качестве эффективной минеральной добавки для повышения прочности при сжатии и оптимизации состава керамического кирпича на основе местного глинистого сырья.

Keywords: ceramic brick, clay raw material, bentonite, clay raw material compressive strength, clay.

Ключевые слова: керамический кирпич, глинистое сырье, бентонит, плотность глинистого сырья, прочность при сжатии, глина.

Introduction

Ceramic brick is one of the most widely used wall-building materials in construction due to its relatively low cost and the possibility of producing it from locally available raw materials. The long-term reliability of buildings and structures largely depends on the mechanical strength, deformation characteristics, water resistance, and durability of bricks under environmental influences [1, 2]. Therefore, improving the physical and mechanical properties of ceramic bricks, efficiently utilizing local raw materials, and determining optimal compositions are important scientific and practical tasks [2, 3, 5]. In the production of ceramic bricks, the technological and performance properties of the material can be controlled by incorporating various mineral additives into the raw material composition [3, 4, 10]. Bentonite clay, in particular, is characterized by a high content of montmorillonite minerals, high dispersity, and binding properties. These characteristics of bentonite may positively influence the interaction between particles in the ceramic mixture, improve the molding process, and contribute to the formation of a dense and strong structure during firing [6, 8].

However, when the amount of bentonite additive is excessively increased, the optimal ratio of mineral components in the ceramic mixture may be disturbed, leading to increased volumetric changes during drying and firing and, consequently, a reduction in the mechanical properties of the bricks [7, 8, 10]. Therefore, not only the presence of bentonite but also the determination of its optimal content is of considerable importance [6, 10]. Establishing the optimal content can make it possible to produce ceramic bricks with higher strength from locally available raw materials while improving production efficiency [3, 6]. Uzbekistan has considerable potential for using locally available soils and clay raw materials in the production of construction materials. At the same time, the mineralogical and chemical composition of local raw materials varies depending on the region

[5, 9]. Therefore, it is necessary to experimentally determine the optimal amount of mineral additives incorporated into such raw materials. In particular, evaluating the effect of different amounts of bentonite clay added to a ceramic mixture based on local soil on the compressive strength of bricks is of practical significance [6].

The main objective of this study is to determine the effect of incorporating different amounts of bentonite clay into ceramic bricks produced from local soil on their physical and mechanical properties and to establish the optimal bentonite content that ensures adequate compressive strength. Within the framework of the study, specimens containing different amounts of bentonite were prepared, and their strength characteristics were compared with those of a control specimen. The results of this study can provide a scientific and practical basis for optimizing the composition of ceramic bricks produced from locally available raw materials with bentonite additives, improving their mechanical strength, and enhancing the technology for manufacturing construction materials. The novelty of this research is the establishment of the optimum amount of bentonite in the production of ceramic bricks from local loess clay soil of the Kosonsoy region (Uzbekistan). The present study is a new research that sets the bentonite dosage which gives the highest compressive strength with this local raw material in industrial production conditions, unlike the previous ones carried out on other clay deposits and raw materials

Materials and methods

During the experimental study, local clay soil was used as the main raw material, while bentonite was used as additional components. The material consumption required for the production of 1,000 conventional ceramic bricks is presented in Table 1.

Table 1.

Material consumption for the production of 1,000 bricks

Material/Parameter	Unit	Value
Soil	m^3	2.7
Soil density	kg/m^3	1640
Soil mass	kg	4428
Ordinary water	L	886

A comprehensive study was conducted to evaluate the effect of partially replacing the local clay soil with bentonite at contents of 3, 6, 9, 12, 15, 18, 21, 24, 27, and 30 % on the physical and mechanical properties of the bricks, particularly their compressive strength. During the study, changes in brick density, porosity, and strength characteristics with increasing bentonite content were evaluated, with the aim of determining the optimal bentonite content. The specimens were prepared in accordance with ГОСТ 530 – 2012, “Ceramic Bricks and Stones,” based on the applicable international standard [11]. The raw material compositions used for the brick specimens are presented in Table 2.

Table 2.

Raw material composition of the brick specimens

Series	Bentonite (%)	Bentonite (kg)	Soil (kg)	Total dry mass (kg)	Ordinary water (L)	Number of specimens
T	-	-	4.428	4.428	0.886	15
T-B-3	3	0.133	4.295	4.428	0.886	15
T-B-6	6	0.266	4.162	4.428	0.886	15
T-B-9	9	0.399	4.029	4.428	0.886	15
T-B-12	12	0.531	3.897	4.428	0.886	15
T-B-15	15	0.664	3.764	4.428	0.886	15
T-B-18	18	0.797	3.631	4.428	0.886	15
T-B-21	21	0.930	3.498	4.428	0.886	15
T-B-24	24	1.063	3.365	4.428	0.886	15
T-B-27	27	1.196	3.232	4.428	0.886	15
T-B-30	30	1.328	3.100	4.428	0.886	15

The preparation and firing of the specimens were carried out mainly at the “Komiljon Muminov” private enterprise, located in Kosonsoy District, which specializes in the production of bricks. The experimental brick specimens were prepared in accordance with the applicable standards using molds with standard dimensions of 250 × 120 × 65 mm. A total of 11 series of experimental specimens were produced to determine the compressive strength characteristics of conventional ceramic bricks. The specimens were dried under natural conditions. Natural drying was carried out indoors for 7 days. During the drying period, the air temperature was maintained at 20–30 °C, with a relative humidity of 60–75 %. The bricks were stored under conditions protected from direct sunlight. The general appearance of the specimens dried under natural conditions is shown in Figure 1.

Figure 1. General appearance of bentonite-based brick specimens dried under natural conditions

After the raw bricks had been naturally dried, they were placed in a kiln for the firing process. The kiln-firing process was aimed at ensuring the final strength and quality of the bricks and was carried out in several stages. The general appearance of the fired brick specimens is shown in Figure 2.

Figure 2. General appearance of the fired brick specimens

First, the kiln was heated gradually. This initial stage typically lasted 8 hours, during which the remaining moisture inside the bricks evaporated. The temperature was controlled within the range of 200-300 °C to prevent the formation of cracks. In the subsequent stage, the temperature was gradually increased to 900-1050 °C, and this stage typically lasted 16 hours. At the end of the firing process, the kiln was gradually cooled, with the cooling process lasting approximately 14 hours. The experimental testing was carried out in the testing laboratory of “Techno Standard Test” LLC.

Before testing, the dimensions of all specimens were measured with an accuracy of 1 mm, and each geometric dimension was determined as the average value of measurements taken on opposite surfaces. During the test, each specimen was positioned at the center of the testing machine platen, with the geometric axes of the specimen and the platen carefully aligned. The specimen was then securely placed between the upper and lower platens of the testing machine. The load was applied to the specimens continuously and uniformly increased throughout the test. The loading rate was selected so that failure of the specimen occurred within 20-60 seconds after the beginning of the test.

Results and discussion

The experimental results indicated that the compressive strength of the ceramic bricks changed in a non-linear way due to the addition of bentonite. With bentonite content increased from 0 to 12 %, the compressive strength was increased gradually and then decreased slightly. The mean compressive strength value of the control specimens was 67.20 kg/cm², while the highest mean compressive strength value obtained was 84.00 kg/cm² at a bentonite content of 12 %, which showed a 25.0 % increase when compared with the control composition. The results from the 15 individual measurements taken for each mixture were analyzed statistically to assess the variability and repeatability of the experimental results. For each bentonite content, the mean value, the standard deviation (SD), the 95 % confidence interval (CI), and the coefficient of variation (CV) were determined. Table 3 shows the results of the statistical analysis.

Table 3.

Statistical characteristics of compressive strength of ceramic brick specimens at different bentonite contents

Bentonite content, %	n	Mean, kg/cm²	SD, kg/cm²	95% CI, kg/cm²	CV, %
0	15	67.20	3.47	65.28-69.12	5.16
3	15	72.58	4.44	70.12-75.04	6.12
6	15	77.95	4.89	75.24-80.66	6.27
9	15	81.98	4.65	79.40-84.56	5.67
12	15	84.00	4.48	81.52-86.48	5.33
15	15	81.66	4.92	78.94-84.38	6.02
18	15	75.30	4.63	72.74-77.86	6.15
21	15	71.26	4.31	68.87-73.65	6.05
24	15	66.56	3.91	64.39-68.73	5.87
27	15	63.84	3.64	61.82-65.86	5.70
30	15	58.20	3.68	56.16-60.24	6.32

The coefficient of variation values were between 5.16 % and 6.32 %, which shows the dispersion of the measured compressive strength values of the replicate specimens was relatively low. The 95 % confidence intervals also illustrate the variability that exists for each mean value. This gives the maximum mean compressive strength for the bentonite content of 12 % bentonite, 81.98 kg/cm² and 81.66 kg/cm², respectively, for the bentonite content of 9 % and 15 %. The experimental results are graphically shown in Figure 3. Error bars show the 95 % confidence interval for each of the 15 replicate measurements for each mixture.

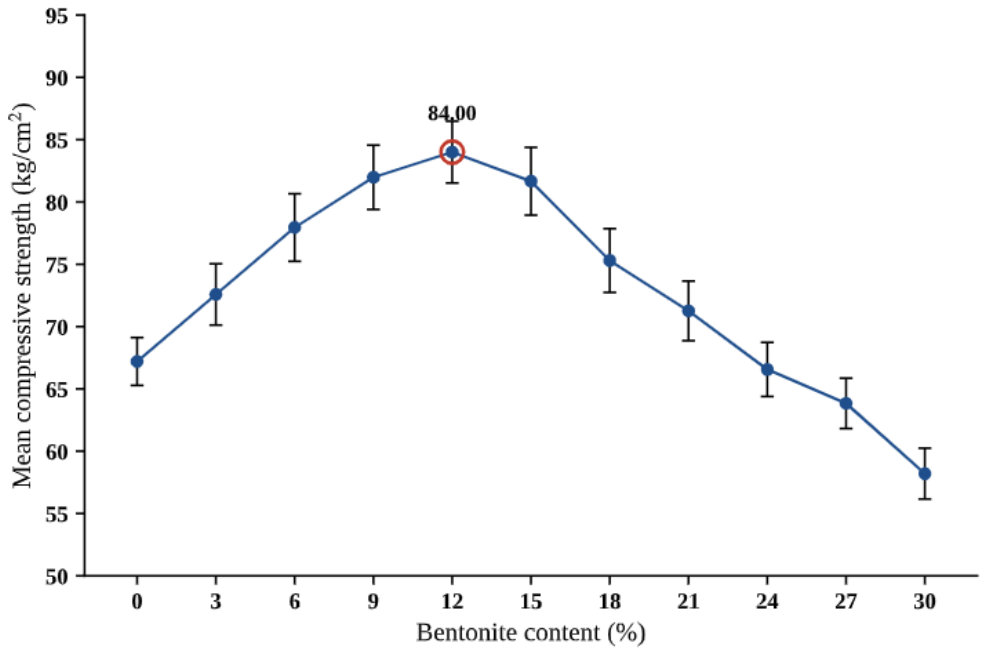

Figure 3. Compressive strength of the specimens

This was due to the increase in compressive strength after adding bentonite to the control composition, which recorded 67.20 kg/cm², while it recorded 72.58, 77.95, 81.98, and 84.00 kg/cm² at bentonite levels of 3, 6, 9, and 12 %, respectively. These values are 8.01 %, 16.00 %, 21.99 %,

and 25.00 % greater than that of the control specimen. At higher bentonite contents, the compressive strength decreased, reaching 81.66, 75.30, 71.26, 66.56, 63.84, and 58.20 kg/cm² at 15, 18, 21, 24, 27, and 30 % bentonite, respectively. The strength of the specimen with bentonite content of 30 % was 13.39 % lower than that of the control specimen.

The observed strength improvement at medium bentonite content may be correlated with the fine and highly dispersed bentonite particles, which could fill interparticle voids in the clay matrix and create a denser ceramic structure after firing. This interpretation should be used in conjunction with the experimental conditions, as the present study did not carry out any direct microstructural or mineralogical analysis. Increased bentonite concentration could lead to a greater amount of swelling clay minerals and higher water requirements of the mixture and enhance drying shrinkage at higher bentonite concentrations. These changes can contribute to the formation of internal defects and microcracks that can negatively influence the compressive strength of the fired ceramic material. Thus, the compressive strength results from the experiments show that the optimum bentonite proportion of 12 % gives the maximum measured strength.

Conclusions

1. The experimental findings indicated that the ceramic bricks made from local clay soil were affected by the addition of bentonite. The compressive strength also rose as bentonite content increased, with peaks at 12 % at the value of 84.0 kg/cm², which is an increase of 25.0 % over the control composition of 67.2 kg/cm². The strength had a tendency to decrease with an increase in bentonite content up to 30 % bentonite, where it reduced to 58.2 kg/cm², which is 13.4 % lower than the control strength.

2. The enhancement of the compressive strength at intermediate bentonite levels might be related to better packing and densification of the ceramic mass during firing. With higher bentonite percentages, the internal defects and the microcracks can be formed due to the increased water demand and shrinkage and may be responsible for the decrease in compressive strength.

3. The main practical value of this work is the determination of the bentonite content, which gives the maximum compressive strength to ceramic bricks manufactured from local loess clay soil of the Kosonsoy region of Uzbekistan. The results obtained in this study show that the optimum bentonite content of the composition is 12 %, which yielded the highest mean compressive strength of 84.0 kg/cm² when compared with the control composition.

References

1. Balksten K., Strandberg-de Bruijn P. Understanding deterioration due to salt and ice crystallization in scandinavian massive brick masonry // Heritage. – 2021. – Vol. 4. – P. 349–370. – DOI: 10.3390/heritage4010022.
2. Chapagain Y.P. et al. A case study on mineralogy and physico-mechanical properties of commercial bricks produced in Nepal // SN Applied Sciences. – 2020. – Vol. 2.
3. Daumova G. et al. Utilization of spent sorbent in the production of ceramic bricks // ChemEngineering. – 2022. – Vol. 6. – DOI: 10.3390/chemengineering6050082.

4. El-Samrah M.G. et al. Investigation of specially designed bentonite samples as potential bricks with better radiation shielding properties // Progress in Nuclear Energy. – 2023. – Vol. 162. – DOI: 10.1016/j.pnucene.2023.104778.
5. Korpayev S. et al. Characterization of three amu-darya basin clays in ceramic brick industry and their applications with brick waste // Materials. – 2021. – Vol. 14. – DOI: 10.3390/ma14237471.
6. El Boukili G. et al. Improving rheological and mechanical properties of non-plastic clay soil from Bensmim region (Morocco) using bentonite additions: Suitability for building application // Journal of Building Engineering. – 2023. – Vol. 63 – URL: https://10.1016/j.jobe.2022.105525. (accessed 27.09.2026)
7. Wang S. et al. Thermal behaviors of clay minerals as key components and additives for fired brick properties: A review // Journal of Building Engineering. – 2023. – Vol. 66 – URL: https://10.1016/j.jobe.2022.105802. (accessed 27.09.2026)
8. Vasić M.V. et al. The study of thermal behavior of montmorillonite and hydromica brick clays in predicting tunnel kiln firing curve // Construction and Building Materials. – 2017. – Vol. 150. – P. 872–879. – DOI: 10.1016/j.conbuildmat.2017.06.068.
9. Mahmoud K.A. et al. Bentonite-clay bricks reinforced with fuel fly ash: Structural and gamma attenuation characterization // Radiation Physics and Chemistry. – 2025. – Vol. 232. – DOI: 10.1016/j.radphyschem.2025.112599.
10. Nurlybayev R.E. et al. An investigation of the effects of additives and burning temperature on the properties of products based on loam // Applied Sciences. – 2022. – Vol. 12. – DOI: 10.3390/app12073352.
11. GOST 530–2012. Ceramic bricks and stones. General specifications. – Moscow: Standartinform, 2013. – 39 P.

ECOLOGY AND SAFETY

ECOLOGY AND TECHNOSPHERE SAFETY

Статья поступила в редакцию: 07.07.2026
Статья принята к публикации: 13.07.2026
Статья опубликована: 28.09.2026

УДК 556.55:574.5

DOI: 10.32743/UniTech.2026.150.9.23166

Integrated hydrological and hydrobiological assessment of reservoirs in the Amudarya delta: implications for sustainable water supply management

Kaipov Islam
Independent Researcher
Scientific Research Institute of Irrigation and Water Problems
Uzbekistan, Tashkent
https://orcid.org/0000-0001-7213-5754
E-mail: i.p.kaipov@gmail.com

Kurbanbaev Sagit
PhD, Senior Researcher, Director
Karakalpak Branch of the Scientific Research Institute of Irrigation and Water Problems
Uzbekistan, Nukus
http://orcid.org/0000-0002-6772-7453
E-mail: kurbanbaev69@mail.ru

Библиографическое описание: Каипов И.П., Курбанбаев С.Е. Комплексная гидрологическая и гидробиологическая оценка водохранилищ в дельте реки Амударья: последствия для устойчивого управления водными ресурсами // Universum: технические науки : электрон. научн. журн. 2026. 9(150). URL: https://7universum.com/ru/tech/archive/item/23166

For citation: Kaipov I., Kurbanbaev S. Integrated hydrological and hydrobiological assessment of reservoirs in the Amudarya delta: implications for sustainable water supply management // Universum: Technical Sciences : electronic scientific journal. 2026. No. 9(150). Available at: https://7universum.com/ru/tech/archive/item/23166

Комплексная гидрологическая и гидробиологическая оценка водохранилищ в дельте реки Амударья: последствия для устойчивого управления водными ресурсами

Каипов Ислам Пердебаевич
независимый исследователь, Научно-исследовательский институт ирригации и водных проблем
Республика Узбекистан, г. Ташкент

Курбанбаев Сагит Ережепович
PhD
ст. науч. сотр., директор, Каракалпакский филиал Научно-исследовательского института ирригации и водных проблем
Республика Узбекистан, г. Нукус

Abstract

Water scarcity and hydrological alterations in the Amudarya Delta have significantly affected the ecological condition and operational efficiency of its major reservoirs. This study presents an integrated assessment of the hydrological and hydrobiological conditions of the Mezhdurechenskoye, Muynak, and Ribachye reservoirs to support sustainable water supply management. Long-term hydrological observations from the Kiziljar gauging station (1965–2022), field surveys, morphometric analysis, and hydrobiological investigations were combined with mathematical modeling of the reservoir water balance. A Visual C#-based model was developed to simulate water balance under high-, average-, and low-water conditions, while ArcGIS was employed to evaluate current morphometric characteristics. The results indicate a persistent decline in river discharge and a reduction of 14–17 % in reservoir surface area and 12–17 % in storage capacity compared with the design parameters. Hydrobiological surveys identified 27 zooplankton species, with the highest biomass recorded in the Mezhdurechenskoye Reservoir due to its relatively stable hydrological regime. Model simulations demonstrate that rehabilitation of the Glavmyaso and Marinkinuzyak canals would substantially improve reservoir replenishment and restore water storage to near-design capacity. The findings provide a scientific basis for optimizing reservoir operation and improving water resources management in the Amudarya Delta under increasing water scarcity and climate change.

Аннотация

Дефицит водных ресурсов и гидрологические изменения в дельте Амударьи существенно повлияли на экологическое состояние и операционную эффективность ее основных водохранилищ. В данном исследовании представлена комплексная оценка гидрологических и гидробиологических условий Междуреченского, Муйнакского и Рыбачьего водохранилищ для поддержки устойчивого управления водоснабжением. Многолетние гидрологические наблюдения на гидропосту Кызылжар (1965–2022 гг.), полевые обследования, морфометрический анализ и гидробиологические исследования были объединены с математическим моделированием водного баланса водохранилищ. Для моделирования водного баланса в условиях высокой, средней и низкой водности была разработана модель на базе Visual C#, а для оценки современных морфометрических характеристик применялась система ArcGIS. Результаты указывают на устойчивое снижение

речного стока, а также на сокращение площади водного зеркала водохранилищ на 14–17 % и их полного объема на 12–17 % по сравнению с проектными параметрами. В ходе гидробиологических съемок было выявлено 27 видов зоопланктона, при этом наибольшая биомасса зафиксирована в Междуреченском водохранилище, что обусловлено его относительно стабильным гидрологическим режимом. Результаты моделирования показывают, что реконструкция каналов Главмясо и Маринкинузяк позволит существенно улучшить наполняемость водохранилищ и восстановить запасы воды до близких к проектным значений. Полученные результаты обеспечивают научную основу для оптимизации работы водохранилищ и совершенствования управления водными ресурсами в дельте Амударьи в условиях растущего дефицита воды и изменения климата.

Keywords: Amudarya Delta, reservoirs, hydrological assessment, hydrobiological assessment, morphometric analysis, water balance modelling, zooplankton, sustainable water management.

Ключевые слова: дельта Амударьи, водохранилища, гидрологическая оценка, гидробиологическая оценка, морфометрический анализ, моделирование водного баланса, зоопланктон, устойчивое управление водными ресурсами.

Introduction

Water resources in arid and semi-arid regions are highly vulnerable to the effects of climate changes and anthropogenic activities, which are exacerbated by growing populations and increasing agricultural water demands. Such problems are especially acute in the Amudarya Delta due to significant declines in river runoff and large-scale deterioration of freshwater ecosystems that have occurred since the 60s of the last century. This has had a major impact on the functioning of reservoirs in the delta, which are vitally important for regulating the river regime and ensuring the viability of the local ecosystem. The present research explores the relationship between changes in hydrological processes and the ecological state of the reservoirs in the Amudarya Delta.

The main sources of water in the Amudarya Delta are the reservoirs of Mezhdurechenskoye, Muynak, and Ribachye, which serve as regulators of seasonal river flows, provide sustainable water supplies to irrigated farms, ensure fish breeding, and maintain the proper ecological state of the estuary part of the river. However, due to long-term water deficits, structural changes in the reservoirs, decreasing channel conveyance capacity, and high rates of evaporation, their water storage capacities have significantly decreased. Moreover, hydrobiological studies have shown that the number and quality of zooplankton species are of great importance for the ecological state of the reservoirs. Previously published studies exploring the ecological and hydrological problems of the Amudarya Delta typically focused on specific areas of water resource management. Therefore, there is a lack of integrated research that would consider the delta’s natural and man-made reservoirs as interconnected systems in the context of long-term changes in water balance, morphology, and water regime. This study aims to fill this gap by providing an in-depth assessment of the physical and ecological characteristics of the three major reservoirs in the Amudarya Delta.

The novelty of this work consists in the combined analysis of hydrological and hydrobiological aspects of the functioning of natural and artificial reservoirs in the Amudarya Delta using long-term observational data, field measurements, GIS technologies, and the mathematical model of the water balance implemented in the programming language Visual C#. The current research will contribute to a better understanding of the processes affecting the water regime and ecological state of the reservoirs in the Amudarya Delta. The primary objective of this study is to assess the hydrological and hydrobiological conditions of the Mezhdurechenskoye, Muynak, and Ribachye reservoir and develop evidence-based recommendations for adjusting water management practices to ensure sustainable water use in the Amudarya Delta.

Materials and methods

The objects of the research were the Amudarya River and the territory of its delta (the Mezhdurechenskoye [17863 ha], Muynak [12529 ha], and Ribachye [6243 ha] reservoirs). The following general categories of methods were used: hydrological (based on a hydrological analysis of the area's characteristics and water balance calculations), GPS-assisted field geodetic surveying, GIS-based morphometric modeling, mathematical water balance modeling, hydrobiological studies (hydrobiological surveys and laboratory analysis of water and biogenic sediment samples), and finally, statistical analysis of uncertainties.

2.1. Hydrological data

Long-term hydrological data were collected from Kiziljar station on the Amudarya River, provided by the Hydrometeorological service of Uzbekistan (Uzhydromet) for the period 1965–2022. The discharge data for the study area are based on standard velocity–area measurements with current meters (GOST 8.361), with a stated accuracy of ±5 % for typical flow conditions. The field measurements were made at the delta reservoirs in 2002, 2018, and 2022.

2.2. Geodetic and GPS field surveys

The field topographic and bathymetric surveys of the Mezhdurechenskoye reservoir (October 2022), Muynak (October 2022), and Ribachye (November 2023) reservoirs were carried out using a Garmin eTrex 10J (010-00970-06) handheld GPS receiver. An optical level and theodolite were used to determine cross-section and shoreline points. Beforehand, the Garmin eTrex 10J GPS receiver was tested against the known coordinates of the permanent benchmark of the State Geodetic Network; the level was checked by the two-peg test, and the theodolite was tested for collimation/index error. Thus, the accuracy of vertical measurements was ±0.05 m, and the horizontal accuracy, according to the Garmin eTrex 10J specifications, was ±3 m. Shoreline and cross-section points were measured using the GPS receiver and checked against the benchmarks to minimize horizontal positioning errors. The cross-sections were spaced at intervals needed to ensure that the reservoirs' primary morphological features were captured.

2.3. GIS-based morphometric modelling

The surveyed points were imported into ArcGIS 10.8, where they were used to generate a TIN representing the reservoirs' bed and shoreforms at the time of surveys following the methodology used in the authors' previous work on delta reservoirs [20]. Using the Surface Volume tool, the surface area and storage volume of the reservoirs were estimated at the level of 57.30 m a.s.l. (Figure 3), which corresponds to the project design level, and were compared to the measured values (Table 1). To estimate the accuracy of interpolated values, a leave-one-out validation was carried out for a 10% subset of measured points. Combined with the GPS/level accuracy (Section 2.2), this allowed the estimation of accuracy of the interpolated volumes and areas presented in Table 1 with an uncertainty of no more than ±3–5%.

2.4. Water balance mathematical model

The surveyed points were imported into ArcGIS 10.8, where they were used to generate a TIN representing the reservoirs' bed and shoreforms at the time of surveys following the methodology used in the authors' previous work on delta reservoirs [20]. Using the Surface Volume tool, the surface area and storage volume of the reservoirs were estimated at the level of 57.30 m a.s.l. (Figure 3), which corresponds to the project design level, and were compared to the measured values (Table 1). To estimate the accuracy of interpolated values, a leave-one-out validation was carried out for a 10 % subset of measured points. Combined with the GPS/level accuracy (Section 2.2), this allowed the estimation of accuracy of the interpolated volumes and areas presented in Table 1 with an uncertainty of no more than ±3–5 %.

A lumped water balance model for the delta reservoir system was constructed as a system of ordinary differential equations and implemented in Visual C # programming language with a monthly computational step (Δt = 1 months):

$$dW/dt = Q_p - q_r - q_E - q_f$$

where Q_p is the flow into the delta, determined by the Samanboy hydrological station (m^3/s), q_r is the channel conveyance loss, here estimated as 25 % of the total flow according to to the established long-term loss coefficients, q_E is the evaporation loss, which is determined for each reservoir on the basis of its active surface area (see Section 2.3) and monthly evaporation data, and q_f is the seepage or filtration loss, estimated on the basis of the properties of the reservoir bottom.

The model was tested for three characteristic years with regard to water availability – 2010 high-water year, 2019 average-water year, and 2001 low-water year for the delta reservoirs – using design and degraded morphometry (initial storage volume set to the field-survey or design value at the beginning of the hydrological year). Series with gaps of more than two consecutive months were completed by linear interpolation; series with more than 20 % of gaps were excluded. The model's performance was evaluated in terms of the deviation of the calculated YEs from the field/ArcGIS YE values (see Section 2.3) at the end of each year, which is detailed in Section 3.1.

Note that while the model describes the functioning of the system as a whole, that is, the inflow into the delta, and operates with a lumped reservoir routing scheme based on the observed flow into the delta and the canal network as a set of discrete structures, a comparison with distributed physically-based models, such as SWAT or MIKE SHE, was not carried out, which is discussed in Section 3.3.

2.5. Hydrobiological surveys and zooplankton analysis

Zooplankton was studied in the reservoirs of the Mezhdurechenskoye, Muynak, and Ribachye cities in 2022 – 2023 – a total of 32 samples were taken. Quantitative samples were taken by passing 100 liters of water through a plankton net (nylon, window size 76), while qualitative ones – by dragging the plankton net. The sampling was carried out in the pelagic zone, in macrophyte vegetation belts, and shallow waters near the coast. All samples were fixed with formalin on site to a concentration of 2 – 3 %. Zooplankton was counted and identified using a microscope and a binocular microscope with temporary and permanent preparations using the methods of T. Kutikova, A. Mordukhai-Boltovskoi, and A. Rylov for the classes Rotifera, Cladocera, and Copepoda, respectively [17-19]. Counting was made in a Bogorov frame with a stamp pipette, and the number of individuals, as well as the biomass, was determined by weight in milligrams per cubic meter based on the average weight of the species given in the literature [17-19]. In addition, water temperature and transparency were measured at the sites using a thermometer and a Secchi disk. Zooplankton data were compared with zoological surveys published previously for the region (Ginatullina et al., 2006 for the Meskhedzha River [9] and Temirbekov et al., 2023 for the Muynak reservoir [16]). At the same time, the literature on the zoology of the former Aral Sea basin was also used as a reference: the works of Nikolskiy [4], Tleuov [11], Pavlovskaya [10], and Qozaqboyev [5] published in the 1940s-1980s, which describe the local zooplankton species composition in detail.

2.6. Statistical processing and uncertainty analysis

The coefficient of variation (Cv) and the coefficient of skewness (Cs) were calculated for the flow series using the Kritsky-Menkel method, which is typical for regionalized hydrological series. Morphometric uncertainty was estimated at ±3 – 5 % due to GPS/altimeter accuracy, and TIN interpolation errors (see Section 2.3). Water balance has two components of uncertainty: an evaporation term and a filtration term, each of which was estimated at ±10 – 15 % (limited by the accuracy of the input data). According to Section 2.1, the discharge measurements have a ±5 % error, which was taken into account when calculating the uncertainty of the balance (Table 2). The number of zooplankton organisms was counted as an average for all stations indicated in Table 3 for the survey dates. The biomass was calculated in mg per cubic meter of water using the average weight of organisms for each species found in the literature (see Section 2.5).

Results and discussion

1. Long-Term Trends in River Discharge

The analysis of hydrological observations at the Kiziljar gauging station for the period 1965–2022 revealed a significant long-term decreasing trend in the Amu Darya discharge in the delta [1]. Thus, the multi-year discharge is on average equal to Q_0 = 177.5 m³/s; the coefficient of variation Cv = 1.08, the coefficient of skewness Cs = 1.79, which indicates a high variability of flow [6]. These values should be considered as approximate since, for the Kiziljar station, the error of the gauging method can be up to ±5 % (Section 2.1). However, the identified trend significantly exceeds this error level. The maximum monthly discharge was noted in 1969 and was equal to 3,530 m³/s, while in individual months in 2001, the discharge was as low as 2.1 m³/s. In the last 30–

35 years, discharges of more than 1,000 m³/s have become significantly less common. Thus, the 3 % exceedance discharge is 714.1 m³/s (1980), the 50 % exceedance discharge is 116.9 m³/s (2000), and the 96 % exceedance discharge is 2.83 m³/s (2021).

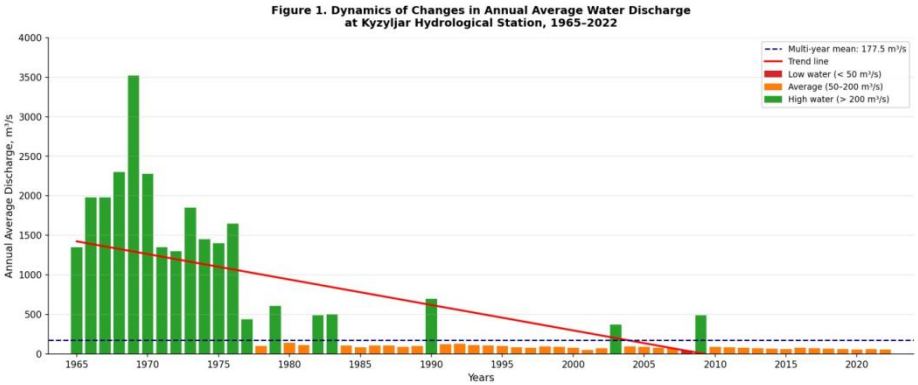

Figure 1. Dynamics of mean annual discharge at Kiziljar gauging station, 1965–2022

2. Morphometric Parameters of the Reservoirs

Field measurements and GIS-based morphometric modeling (see Section 2.3) allowed us to assess present-day morphometric parameters of the Mezhdurechenskoye reservoir (October 2022) and the Muynak and Ribachye reservoirs (November 2023) [7]. According to the field measurements, at the design level of 57.30 m a.s.l., the Mezhdurechenskoye reservoir's total storage is 190.9 million m 3, while according to ArcGIS TIN modeling, it is 230.8 million m 3 . At present, its surface extends over 17,863 ha, which is 16.7 % less than the design size of 21,436 ha. The Muynak reservoir's surface area is 12,529 ha, which is 16.7 % less than the design size of 15,034 ha. Its total storage is 184.9 million m 3, which is 12.8 % lower than the design value of 210 million m 3 . As for the Ribachye reservoir, its surface area is 6,243 ha, compared to the design size of 7,304 ha, and its total storage is 124.9 million m 3, compared to the design value of 151.4 million m 3 . Thus, with the combined measurement uncertainty of 3 – 5 % (see Section 2.3), the decrease in the surface area of all three reservoirs by 14 – 17 % and the total storage by 12 – 17 % is obvious.

Table 1.

Morphometric parameters of principal reservoirs in the Amudarya Delta. Area and volume values carry an estimated combined uncertainty of ±3–5% (see Section 2.3)

Parameter	Mezhdurechenskoye	Muynak	Ribachye	Total / Average
Design area, ha	21,436	15,034	7,304	43,774
Current area, ha	17,863	12,529	6,243	36,635
Reduction, %	16.7%	16.7%	14.5%	16.3%
Design volume, million m³	230.0	210.0	151.4	591.4
Current volume, million m³	191.0	184.9	125.0	500.9
Maximum depth, m	5–6	4.0–4.2	3.5–4.0	—
Mean depth, m	0.5–1.2	1.48	2.0	—
Design channel capacity, m³/s	—	44 (Glavmyaso)	50 (Marinkin)	—
Current channel capacity, m³/s	—	15	20	—

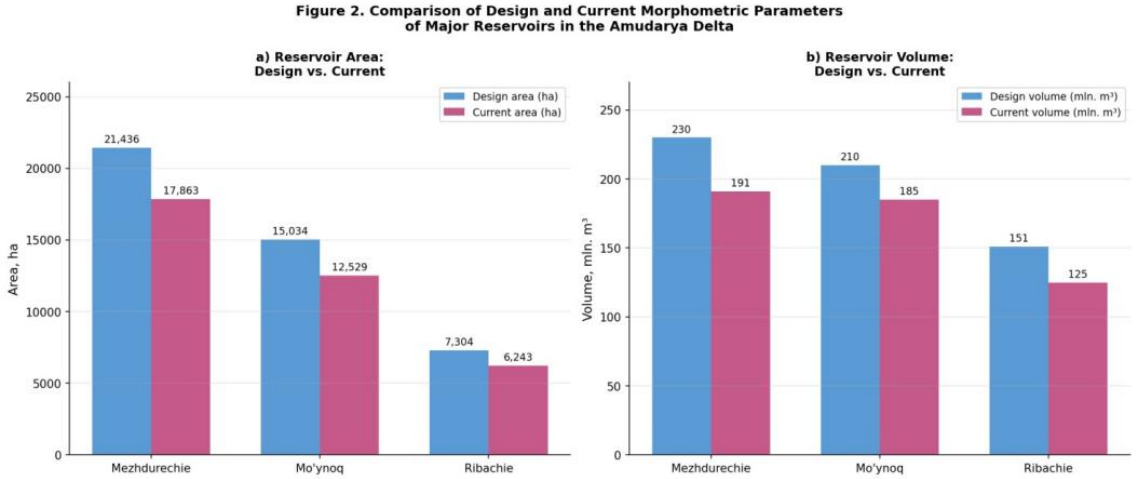

Figure 2. Comparison of design and current morphometric parameters of principal reservoirs in the Amudarya Delta

3. Water Balance and Mathematical Modelling

By using the water balance model described in Section 2.4, calculations were carried out for 2010, which is a high-water year, 2019, which is an average-water year, and 2001, which is a low-water year, with the Visual C#. net implementation of the algorithm for both design and current conditions.

Table 2.

Water balance of the near-Amudarya region for years of differing water availability. Evaporation and filtration losses are shown with the estimated ±10–15% relative uncertainty described in Section 2.6; discharge-derived terms carry the ±5% gauging uncertainty noted in Section 2.1

Parameter	High-water (2010)	Average-water (2019)	Low-water (2001)	Unit
Total inflow (Samanboy g/s)	16,817.7	1,674.4	100.9	million m³/year
Channel losses	4,204.4	418.6	25.2	million m³/year
Total evaporation (all reservoirs)	14.5 ± 1.5–2.2	11.4 ± 1.1–1.7	4.95 ± 0.5–0.7	million m³/year
Filtration losses	1.30 ± 0.13–0.20	1.14 ± 0.11–0.17	0.45 ± 0.05–0.07	million m³/year
Discharge to Aral Sea	12,214.9	852.4	0.0	million m³/year
Water retained in reservoirs	499.98	500.03	218.8	million m³

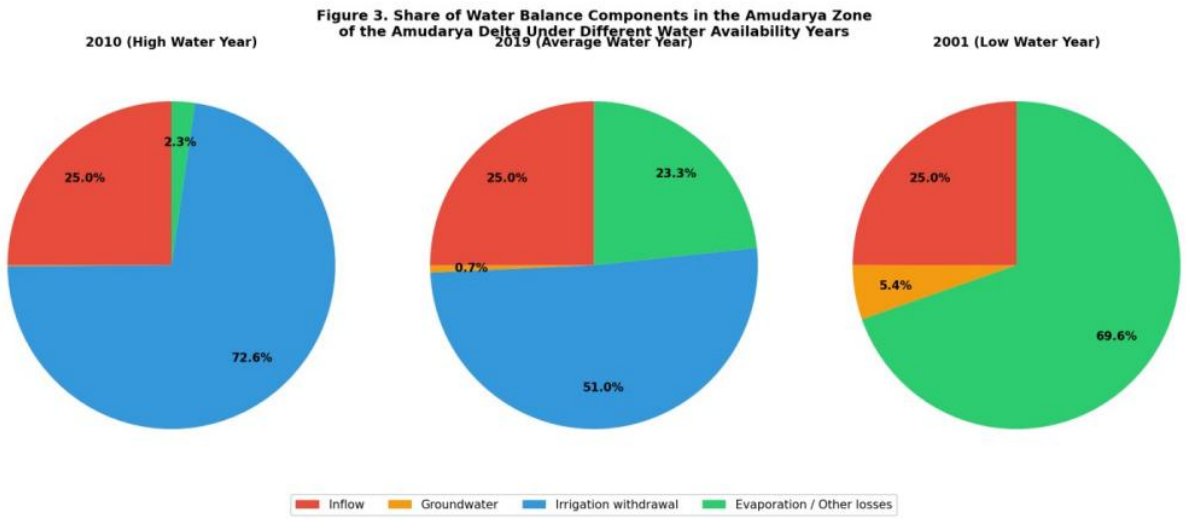

Figure 3. Proportional distribution of water balance components in the Amudarya Delta for years of differing water availability

In the year of high discharge, 2010, the total inflow was 16817.7 million m³, of which 79.8 % was discharged through the channels into the former Aral Sea bed. In the year of average discharge, 2019, the inflow of 1674.4 million m³ allowed to keep the storage of all three reservoirs above 500 million m³. In the year of low discharge, 2001, the inflow was as low as 100.9 million m³, which is by an order of magnitude less than the combined storage of the three reservoirs (currently, 230 + 139 + 151 = 520 million m³). Reconstruction of the canal infrastructure (restoration of the discharge of the Glavmyaso Canal to 44 m³/s and the Marinkinuzyak Canal to 50 m³/s) would allow to fill the Mezhdurechenskoye Reservoir (230 million m³) to full capacity and partially refill the Muynak (139 million m³) and Ribachye (151 million m³) reservoir to their design volumes [8], given the ±10 – 15 % error margins of the evaporation / filtration terms (Section 2.6). This conclusion is not affected by the ±10 – 15 % error margins of the model's input parameters.

3.1. Model verification

The design volumes used in the model as target values for the reservoirs (230.0 million m³ for Mezhdurechenskoye at NPU 57.30 m, 139.0 million m³ for Muynak at NPU 54.50 m, and 151.0 million m³ for Ribachye at NPU 54.00 m) are standard for the respective reservoirs and were verified against the current storage volumes found in the field / in ArcGIS in Section 2.3. A quantitative verification of the model (Nash-Sutcliffe efficiency, RMSE compared to an independent storage time series) was not carried out in this study but is recommended for future work when multi-annual reservoir storage time series become available.

3.2. Economic and institutional considerations

A full economic feasibility analysis of the proposed measures was beyond the scope of this hydrological / hydrobiological study, as it would require detailed engineering and surveying work that was not available to the authors. However, as shown in Table 2, the reconstruction of the canals would allow to fill the Mezhdurechenskoye Reservoir and partially refill the Muynak and Ribachye reservoirs to their design volumes even in the year of average discharge, thus ensuring the water supply for irrigation, fisheries, and reducing the need for costly alternative measures in other parts

of the delta. The creation of a water management consortium and the development of water user associations as a mechanism for basin-level resource management [21] could be considered as an institutional solution to the problem. An economic assessment of the proposed solution, balancing the costs of the reconstruction with the benefits from the creation of the reservoirs, is recommended for future research.

3.3. Sensitivity to climate change

The decreasing trend in the mean annual discharge and the increasing trend in its variability observed in the 1965 – 2022 discharge series (Cv = 1.08) could be consistent with the climate change scenario for the region, which involves a temperature rise and a decrease in snow and glacial meltwater resources in the upper reaches of the Amudarya River. In such a scenario, the number of years with low discharge (similar to 2001, see Table 2) will increase, which will reduce the filling rates of the reservoirs to the levels indicated in Table 2 even after the proposed measures. A quantitative analysis of the impact of climate scenarios on the inflow to the reservoirs (using downscaled climate projections as input) was not carried out in this study but is recommended for future research. Given the relatively simple structure of the model used (Section 2.4), the easiest way to implement this analysis would be to use a lumped conceptual model (e. g., SWAT or MIKE SHE) that explicitly considers the impact of climate change on the catchment areas of the reservoirs. This approach would be more resource-intensive but would provide more insight into the sensitivity of the reservoirs to climate change; a combined analysis using the model described in this study and a distributed model is recommended for future research.

4. Hydrobiological Investigations (Zooplankton)

During the 2022 – 2023 field season, 32 zooplankton samples (23 quantitative and 9 qualitative) were taken in the lower reaches of the Amudarya River reservoirs, following the procedure described in Section 2.5. In total, 27 species of zooplankton were found, including 15 species of Rotifera (55.6 %), 6 species of Cladocera (22.2 %), and 6 species of Copepoda (22.2 %) [9].

Table 3.

Zooplankton species richness in lower Amudarya reservoirs (2022–2023), based on the sampling protocol described in Section 2.5

Reservoir	Summer 2022	Autumn 2022	Summer 2023	Autumn 2023
Mezhdurechenskoye	14	9	14	8
Ribachye	—	—	6	—
Muynak	—	—	11	—
Total	14	9	31	8

The largest number of zooplankton species (27 species in total) was found in the Mezhdureschenskoye reservoir. In the Ribachye and Muynak reservoirs, zooplankton were studied only in summer 2023, due to the limited water levels. The greatest number of zooplankton was found in August: 4,400 mg/m 3 in the Mezhdureschenskoye reservoir, 231 mg/m 3 in the Ribachye reservoir, and 124 mg/m 3 in the Muynak reservoir (mean values for stations; section 2.5). Of these,

96 % were copeods (Copepoda). In the lower reaches of the Amudarya reservoirs, seven species of zooplankton were detected for the first time: Hexarthra mira, Asplanchna sieboldi, Polyarthra vulgaris, Bdelloida gen. sp., and other species. However, Keratella tropica, Thermocyclops vermifer, and some other species recorded in the study by Ginatullina et al. (2006) were not found.

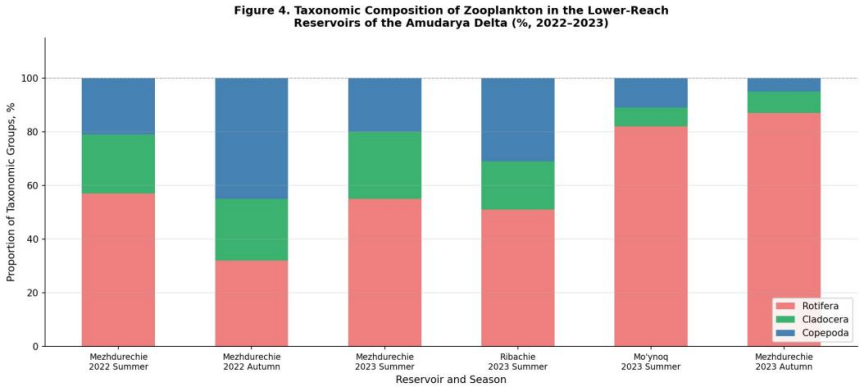

Figure 4. Taxonomic composition of zooplankton in lower Amudarya Delta reservoirs (%, 2022–2023)

Conclusion

1. A systematic decline in Amudarya discharge at Kiziljar station was recorded over 1965–2022, with a mean flow of 177.5 m³/s and Cv = 1.08; the marked decrease in peak discharges over recent decades has substantially reduced water reaching the delta reservoirs.

2. Field measurements and ArcGIS-based TIN modelling (Section 2.3) confirmed that current morphometric parameters of all three reservoirs fall below design by 14–17 % in area and 12–17 % in volume — well outside the estimated ±3–5 % measurement uncertainty — reflecting significant sedimentation and hydrological degradation.

3. The water balance model, developed and verified against field/ArcGIS-derived storage values (Sections 2.4, 3.1), demonstrates that reconstructing the Glavmyaso and Marinkinuzyak canals would restore reservoirs to near-design storage capacity, though its economic justification requires a dedicated cost–benefit analysis (Section 3.2) beyond the scope of this study.

4. Hydrobiological surveys, using the sampling protocol described in Section 2.5, identified 27 zooplankton species across the reservoirs. Mezhdurechenskoye showed the greatest diversity and highest biomass (4,400 mg/m³), reflecting its more stable regime; productivity declines sharply in low-water years, indicating ecosystem vulnerability.

5. The observed increase in discharge variability over 1965–2022 suggests that climate-driven declines in Amudarya flow may reduce the long-term effectiveness of canal reconstruction alone, underscoring the need for climate-scenario modelling in future planning (Section 3.3).

6. The research findings have been implemented at the Priaralie Delta Directorate under the Ministry of Water Resources of the Republic of Karakalpakstan and at the Nukus branch of the International Fund for Saving the Aral Sea.

References

1. Rogov M.M. Hydrology of the Amu Darya Delta. – Leningrad: Gidrometeoizdat, 1957. – 254 P.

2. Dukhovny V.A. Water and Environmental Stability in Central Asia // Problems of the Aral Sea and the Aral Sea Region. – 2008. – P. 4–13.
3. Dukhovny V.A., Sokolov V.I. Basic Provisions of the Concept of Integrated Management // Proceedings of the Scientific Conference of Scientific Center of International Water Commission. – 2012. – P. 11–14.
4. Nikolsky G.V. Fishes of Central Asia. – Moscow: Publishing House of the USSR Academy of Sciences, 1940. – 289 P.
5. Qozaqboyev S. Biologiya i ekologiya planktonnyh rakoobraznyh yuzhnogo Arala. – Nukus: Bilim, 1986. – 120 P.
6. Kurbanbaev S.E. Changes in the hydrological regime… in the Amu Darya River delta // Geographical Society of Uzbekistan. – 2009. – No. 34. – P. 153–156.
7. Kaipov I. Analysis of the hydrological regime and morphometric characteristics of the Mezhdurechenskoye reservoir // «Orolbo'yi hududida iqlim o'zgarishi va suv tanqisligi sharoitida qishloq xo'jaligini rivojlantirishning innovatsion texnika va texnologiyalari» mavzusidagi xalqaro ilmiy va ilmiy-texnik konferensiyasi materiallar to'plami. – 2026.
8. Kaipov I. Amudaryo quyi oqimi gidrotexnik inshootlarining suv balansi dinamikasi va ekologik barqarorlik masalalari (Mejdurechie suv ombori misolida) // «Orolbo'yi hududida iqlim o'zgarishi va suv tanqisligi sharoitida qishloq xo'jaligini rivojlantirishning innovatsion texnika va texnologiyalari» mavzusidagi xalqaro ilmiy va ilmiy-texnik konferensiyasi materiallar to'plami. – 2026.
9. Ginatullina E.N. va boshq. Zooplankton Mezhdurechenskogo vodoxranilishcha i ozer Muynak i Rybachye // O'zbekiston biologiya jurnali. – 2006. – No. 4.
10. Pavlovskaya L.P. Sistematika, ekologiya i ohrana ryb nizoviy Amudar'i. – Toshkent: Fan, 1984.
11. Tleuov R. Biologiya karpovyh ryb yuzhnogo Priaral'ya. – Nukus: Qaraqalpaqstan, 1979.
12. O'zbekiston Respublikasi Prezidentining 2021 yil 29 iyuldagi PQ-5202-son qarori «Orolbo'yi mintaqasini ekologik innovatsiyalar va texnologiyalar hududi deb e'lon qilish to'g'risida». – Toshkent, 2021.
13. Kurbanbaev E., Artykov O., Kurbanbaev S.E. Integrated Water Resources Management in the Amu Darya River Delta. – Tashkent. – 2010. – 156 P.
14. Kurbanbaev S.E. Changes in the Hydrographic Network of the Amu Darya River Delta // Bulletin of the Krasnodar Krai Branch of the Academy of Sciences of the Republic of Uzbekistan. – 2015. – No. 1. – P. 14–19.
15. Kurbanbaev E., Kurbanbaev S.E. Determination of the Expected Income of Maximum Discharges // Bulletin of the Krasnodar Krai Branch of the Academy of Sciences of the Republic of Uzbekistan. – 2015. – No. 2. – P. 24–27.
16. Temirbekov R., Mirzambetov N., Musaev A., Israilova I., Kaipov I., Turlibaev Z. Current state of biodiversity and hydrological-hydrochemical regime of the Mezhdurechensk reservoir of the Republic of Karakalpakstan // IOP Conference Series: Earth and Environmental Science. – 2023. – Vol. 1284. – DOI: 10.1088/1755–1315/1284/1/012007.

17. Kutikova L.A. Rotifers of the USSR Fauna (Subclass Eurotatoria). – Leningrad: Nauka, 1970. – 744 P.
18. Mordukhai-Boltovskoi F.D. (ed.) Identification Guide of Freshwater Invertebrates of the European Part of the USSR (Plankton and Benthos). – Leningrad: Hydrometeoizdat, 1970.
19. Rylov V.M. Freshwater Cyclopoida. Fauna of the USSR, Crustacea, Vol. III, No. 3. – Moscow; Leningrad: USSR Academy of Sciences, 1948.
20. Kaipov I.P., Kurbanbaev S.E. Amudaryo deltasi suv havzalarini GIS texnologiyalari yordamida gidrologik baholash va boshqarish istiqbollari // «Geodeziya, kartografiya va geoinformatika» ilmiy-texnik jurnali. – 2026. – DOI: 10.5281/zenodo.21337621.
21. Kurbanbaev S.E., Kaipov I.P., Turlybaev Z.T. Rational management of water resources in the Amu Darya delta through the creation of a consortium // Me'morchilik va Qurilish muammolari (ilmiy-texnik jurnal). – 2025. – No. 1.

Статья поступила в редакцию: 20.06.2026
Статья принята к публикации: 03.07.2026
Статья опубликована: 28.09.2026

УДК 539.14+543.06

DOI: 10.32743/UniTech.2026.150.9.23393

Nuclear-physical methods for analyzing the elemental composition of samples of man-made and environmental objects

Kurbanov Bakhtiyar Ibragimovich
professor
Institute of Nuclear Physics of the Academy of Sciences of the Republic of Uzbekistan
Uzbekistan, Tashkent
E-mail: kurbanov_1960@bk.ru
Jurakulov Alisher Rustamovich
Associate Professor
Department of General Physics, Navoi State Mining and Technological University
Uzbekistan, Navoi
E-mail: ali_80_84@mail.ru
Muzafarov Amrullo Mustafoevich
professor
Department of General Physics, Navoi State Mining and Technological University
Uzbekistan, Navoi
E-mail: a.muzafarov@gmail.com
Danilova Yelena Artavazdovna
Senior scientific worker Institute of Nuclear Physics of the Academy of Sciences of the Republic of Uzbekistan; Uzbekistan, Tashkent
E-mail: danilova49@mail.ru
Urunov Isokul Oblokulovich
Associate Professor
Department of General Physics, Navoi State Mining and Technological University
Uzbekistan, Navoi
E-mail: isakulurunov@gmail.com

Библиографическое описание: Ядерно-физические методы анализа элементного состава проб техногенных и экологических объектов // Universum: технические науки : электрон. научн. журн. Курбанов Б.И. [и др.]. 2026. 9(150). URL: https://7universum.com/ru/tech/archive/item/23393

For citation: Nuclear-physical methods for analyzing the elemental composition of samples of man-made and environmental objects // Universum: Technical Sciences : electronic scientific journal. Kurbanov B.I. et al. 2026. No. 9(150). Available at: https://7universum.com/ru/tech/archive/item/23393

Ядерно-физические методы анализа элементного состава проб техногенных и экологических объектов

Курбанов Бахтияр Ибрагимович
проф.
Института ядерной физики Академии наук РУз
Республика Узбекистан, г. Ташкент
Журакулов Алишер Рустамович
доц. кафедры Общая физики
Навоийский государственный горно-технологический университет
Республика Узбекистан, г. Навои
Музафаров Амрулло Мустафоевич
проф. кафедры
Общая физики Навоийский государственный горно-технологический университет
Республика Узбекистан, г. Навои
Данилова Елена Артаваздовна
ст. научн сотр. Института ядерной физики Академии наук РУз
Республика Узбекистан, г. Ташкент
Урунов Исокул Облакулович
проф. кафедры
Общая физики, Навоийский государственный горно-технологический университет
Республика Узбекистан, г. Навои

Abstract

This paper presents the application of nuclear-physical methods for determining the elemental composition of samples collected from technogenic objects and environmental media. The study focuses on the use of instrumental neutron activation analysis (INAA), prompt gamma neutron activation analysis (PGNAA), and gamma activation analysis (GAA) for qualitative and quantitative determination of macroelements, trace elements, and technologically significant components in ores, soils, rocks, waters, and industrial products. Experimental investigations were carried out using the VVR-SM research reactor and high-resolution HPGe gamma spectrometers at the Institute of Nuclear Physics of the Academy of Sciences of the Republic of Uzbekistan. Certified reference materials, including IAEA-336 Lichen, IAEA-375 Soil, and NIST SRM 1572 Citrus Leaves, were used to verify the accuracy and reliability of the analytical procedures. The obtained results demonstrated good agreement with certified values and confirmed the high sensitivity, selectivity, and reliability of the applied methods. The elemental composition of samples collected from technogenic territories of Uzbekistan was determined, and the concentrations of environmentally significant and toxic elements were evaluated. The study also assessed the analytical capabilities, detection limits, and practical applicability of neutron-radiation and gamma-activation methods for environmental monitoring, geological exploration, and technological process control in mining and metallurgical industries.

Аннотация

В данной работе представлены результаты применения ядерно-физических методов анализа элементного состава проб техногенных объектов и компонентов окружающей среды. Основное внимание уделено использованию инструментального нейтронно-активационного анализа (ИНАА), нейтронно-радиационного метода анализа и гамма-активационного анализа

для качественного и количественного определения макро-, микроэлементов и технологически значимых компонентов в рудах, почвах, горных породах, водах и продуктах переработки минерального сырья. Экспериментальные исследования выполнены на базе исследовательского реактора ВВР-СМ Института ядерной физики Академии наук Республики Узбекистан с применением современных гамма-спектрометрических систем на основе полупроводниковых HPGe-детекторов. Для оценки точности и достоверности результатов использованы сертифицированные стандартные образцы IAEA-336 Lichen, IAEA-375 Soil и NIST SRM 1572 Citrus Leaves. Полученные результаты показали хорошее соответствие сертифицированным значениям и подтвердили высокую чувствительность, селективность и надежность применяемых методов. Определён элементный состав образцов, отобранных на территориях техногенных объектов Узбекистана, а также проведена оценка содержания токсичных и экологически значимых химических элементов. Установлены пределы обнаружения и аналитические возможности исследованных методов, что подтверждает перспективность их использования для экологического мониторинга, геологоразведочных работ и аналитического контроля технологических процессов горно-металлургической промышленности.

Keywords: Elemental composition, atomic nucleus, nuclear-physical methods, photonuclear reaction, gamma radiation, spectrometry, detector.

Ключевые слова: Элементный состав, атомное ядро, ядерно-физические методы, фотоядерная реакция, гамма-излучения, спектрометрия, детектор.

Introduction

The elemental composition is a fundamental characteristic of a substance that determines its properties, structure, and the nature of physical, chemical, biological, technological, and other processes. To date, a wide range of methods has been developed and applied to analyze and control the composition of substances in various states. The current level of scientific and technological advancement makes it possible to determine both trace and major quantities of elements in natural, environmental, biological, and technogenic objects [5, 7].

However, in practice, analytical procedures are always subject to specific requirements, such as analysis time, sensitivity, location, and cost, which significantly limit the number of methods suitable for solving a particular analytical task. As a result, many scientific and industrial problems cannot yet be fully addressed using existing analytical techniques. For instance, the issue of providing efficient analytical support for geological exploration and prospecting activities remains insufficiently resolved.

A particularly critical challenge is the analytical control of technological processes in the mining and metallurgical industry. This is associated with the development of automated process control systems, the introduction of new technologies, and increasing demands for product quality and production efficiency. In this context, methods for analyzing and controlling the composition of substances based on nuclear-physical principles can play a significant role in solving these problems.

The study focuses on the use of instrumental neutron activation analysis (INAA), prompt gamma neutron activation analysis (PGNAA), and gamma activation analysis (GAA) for qualitative and quantitative determination of macroelements, trace elements, and technologically significant components in ores, soils, rocks, waters, and industrial products.

Materials and methods

Main Nuclear-Physical Methods for Elemental Analysis of Technogenic and Environmental Samples

Due to its electrical neutrality and other unique properties, the free neutron exhibits a wide range of interactions with atomic nuclei. In particular, it can easily penetrate the nucleus and induce various nuclear transformations. The interaction of a neutron with a nucleus may lead to several types of processes, including elastic scattering (n, n), inelastic scattering (n, n′), reactions accompanied by the emission of multiple neutrons such as (n, 2n) and (n, 3n), reactions with the emission of charged particles (n, p) and (n, α), radiative capture (n, γ), and nuclear fission (n, f) [8, 9].

Each of these nuclear reactions can be utilized for determining the concentration of specific chemical elements in complex compounds. Among the most widely used nuclear-physical methods for elemental analysis under neutron irradiation is instrumental neutron activation analysis (INAA). In addition, other nuclear-physical analytical techniques are of considerable interest, including methods based on prompt gamma-ray spectrometry of neutron capture (often referred to as neutron capture gamma analysis) and methods based on photonuclear reactions induced by bremsstrahlung radiation, known as gamma activation analysis (GAA) [1, 3, 6].

Instrumental Neutron Activation Analysis (INAA)

Neutron activation analysis of the elemental composition of complex samples, when performed using research nuclear reactors and modern gamma spectrometers based on high-purity germanium (HPGe) semiconductor detectors, enables the determination of concentrations of more than 40 elements in soil, plants, water, food products, and human biological substrates (e.g., hair) with high sensitivity.

The use of high-resolution gamma spectrometers equipped with HPGe detectors significantly expands the range of detectable elements, reduces detection limits, and increases analytical throughput.

Application of INAA for Macro and Microelement Analysis

The application of instrumental neutron activation analysis (INAA) for macro- and microelement determination was carried out at the Laboratory of Ecology and Biotechnology of the Institute of Nuclear Physics of the Academy of Sciences of the Republic of Uzbekistan. The experimental facility includes a VVR-SM type research nuclear reactor with a thermal power of 10 MW.

The gamma spectrometric system is based on a high-purity germanium (HPGe) semiconductor detector with an energy resolution of 1.8 keV at the 1332 keV gamma line of ^{60}Co and a relative efficiency of 20 %. The use of such a detector enables the separation of elements with closely spaced gamma energies. For example, zinc and scandium (1115.5 and 1120.5 keV, respectively), as well as magnesium and manganese (843.8 and 846.7 keV), can be resolved and quantified independently based on their distinct peaks without mutual spectral interference.

This significantly improves the sensitivity and accuracy of elemental determination, which is particularly important for the analysis of scandium and zinc in soils, as well as magnesium and manganese in biological samples.

Soil samples collected from technogenic regions of Uzbekistan were prepared for analysis using standard procedures. The collected samples were homogenized, dried, ground, and sieved. Representative subsamples were prepared using the quartering method. For neutron activation analysis, sample masses of 20 – 30 mg were used for short-lived isotopes, while 50 – 70 mg samples were prepared for medium- and long-lived isotopes.

The weighed samples were hermetically sealed in labeled polyethylene containers and irradiated in the neutron flux of the VVR-SM reactor. The irradiated samples were subsequently analyzed using the gamma spectrometric measurement system of the Laboratory of Ecology and Biotechnology at the Institute of Nuclear Physics.

To determine elemental concentrations via radionuclides with different half-lives, various analytical time regimes were applied, including irradiation time, decay (cooling) time, and measurement time. Based on the analysis of characteristic gamma spectra of the activated samples, optimal conditions were selected.

Determination of Elements via Short-Lived Radionuclides

The investigated samples, together with reference standards, were placed in polyethylene containers and irradiated in the vertical channel of the reactor with a neutron flux of 5×10^{13} n/cm²·s for 30 seconds.

The induced activity was measured three times: 10 minutes after irradiation for the determination of magnesium and chlorine, and 4 hours after irradiation for sodium, copper, potassium, and manganese. The determination of copper in soil and plant samples was additionally performed on the following day. The counting time for each measurement ranged from 200 to 300 seconds.

Determination of Elements via Medium-Lived Radionuclides

For the determination of calcium, bromine, lanthanum, gold, uranium, and other elements, the samples were wrapped in aluminum foil and irradiated in the reactor’s wet channel for 20 hours. The induced activity was measured 10 days after irradiation based on the characteristic gamma emissions of the corresponding radionuclides. The counting time for each sample ranged from 200 to 300 seconds.

Determination of Elements via Long-Lived Radionuclides

For the determination of elements via long-lived radionuclides, samples irradiated for 20 hours were measured 30 days after irradiation using their corresponding gamma lines. This methodology made it possible to determine the concentrations of cerium, thorium, chromium, cesium, nickel, iron, zinc, and other elements.

Quality Control and Validation Using Reference Materials

At present, one of the most reliable approaches for verifying the accuracy of analytical results is the use of certified reference materials (CRMs). The most robust validation involves either the certification of newly developed international reference materials or the analysis of existing CRMs with compositions unknown to the analyst. Independent validation of analytical results by internationally recognized organizations is of particular importance.

Experimental Results and Discussion

To assess the accuracy of the developed and applied methodology, the following reference materials were used: IAEA-336 (Lichen), NIST SRM 1572 (Citrus Leaves), and IAEA-375 (Soil). The results of the analysis of these reference materials are presented in Table 1.

Table 1.

Comparison of Experimental Results with Certified Reference Values NIST Standard Reference Material 1572 - CITRUS LEAVES

Elements	**As**	**Ba**	**Br**	**Cl**	**Cr**	**Fe**	**Mn**
Certified value	3.1±0.3	21±3	8.2±0.5	414±25	0.8±0.2	90±10	23±2
Determined	2.9	25	7.9	400	0.76	87	21
Elements	**Ni**	**Rb**	**Na**	**Sc**	**Sr**	**Zn**	-
Certified Value	0.6±0.3	4.84±0.6	160±20	0.01	100±2	29±2	-
Determined	0.68	4.9	162	0.009	110	31	-

As can be seen from the results presented in Table 1, the methodologies developed in the laboratory demonstrate a high level of agreement with the certified values and can be reliably applied in neutron activation analysis of natural samples. To assess the environmental conditions in areas surrounding industrial facilities, the elemental composition of soils and water from technogenic regions of Uzbekistan was investigated using neutron activation analysis. This method enables the determination of a large number of elements in various types of samples with exceptionally high sensitivity. To graphically illustrate the agreement between the determined and certified values, the data from Table 1 are presented in Figure 1.

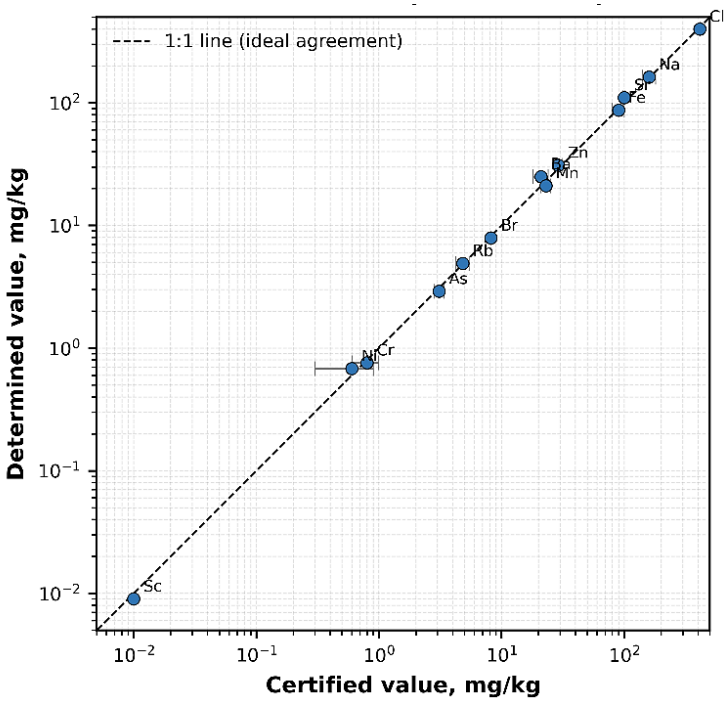

Figure 1. Determined versus certified values for NIST SRM 1572 (Citrus Leaves), plotted on a log-log scale with the 1:1 reference line indicating ideal agreement

As shown in Figure 1, all data points lie close to the 1:1 line across more than four orders of magnitude, confirming the consistency of the developed methodology over a wide concentration range.

The results of the analysis of rock samples collected from territories surrounding technogenic objects in Uzbekistan, obtained using INAA, are presented in Table 2.

Table 2.

NAA Results for Samples from Technogenic Areas of Uzbekistan

Elements	1	2	3	4	5	6	7	8	9	10
Sm	5.88	4.6	6.8	5.04	3.73	4.0	5.19	6.56	4.58	3.92
Mo	3.3	3.08	2.0	1.7	3.97	3.53	2.48	2.33	3.1	1.66
Lu	0.26	0.3	0.35	0.3	0.34	0.35	0.35	0.334	0.29	0.385
U	3.2	10.5	5.15	6.26	8.0	5.06	5.6	5.89	4.35	5.17
Yb	2.38	2.7	2.96	2.54	2.89	2.83	3.13	2.92	3.65	3.34
Au	0.007	0.0072	0.01	0.003	0.0086	0.0095	0.014	0.0098	0.004	0.009
Nd	18.23	26.57	31	24.56	25.52	34.54	42.1	35.61	24.76	39.93
As	7.19	9.1	9.94	9.5	2.1	7.23	8.75	7.54	7.64	8.4
Br	5.3	4.22	4.22	2.75	2.06	4.37	2.27	5.52	3.83	6.36
Ca	2.14	9.73	3.07	6.72	8.87	7.48	10.38	7.97	7.54	9.55
La	26.83	32.52	25.1	32.1	36.13	38.8	38.64	39.66	29.8	38.3
Ce	41.55	54.54	62.9	54.34	60.57	64.2	65.5	64.89	52.29	65.5
Tb	0.51	0.54	0.64	0.49	0.69	0.64	0.73	0.78	0.58	0.69
Th	8.01	24.81	12.01	8.76	25.15	9.53	11.99	13.58	9.53	10.79
Cr	41.74	62.34	67.5	60.74	60.7	60.98	70.87	38.67	67.83	62.9
Hf	3.69	3.98	4.09	4.65	4.83	4.95	5.99	5.51	3.7	8.42
Ba	1581	1159	1321	1257	1048	1336	1051	1130	1386	788.8

Elements	1	2	3	4	5	6	7	8	9	10
Sr	243	401	229	393	363	211	241	246	340	479.36
Cs	4.69	7.86	8.05	7.31	7.1	6.94	7.58	6.79	6.7	6.3
Ni	13.41	28.7	19.54	19.2	25.61	24.66	24.1	24.47	19.19	18.42
Sc	8.62	10.76	10.91	9.93	10.22	10.71	10.72	9.96	10.24	9.63
Rb	57.72	110	122	119	91.33	110	122	109	102.72	92.1
Fe	22948	31253	31403	28766	29358	29416	30713	30206	29534	28732
Zn	117.9	115	112	98	138	107	117	108	108	96.77
Co	8.79	12	11.7	9.67	11.2	10.2	11.27	10.7	11.35	10.75
Ta	0.59	0.81	1.05	0.86	1.07	0.88	1.12	1.03	1.05	1.14
Eu	0.84	0.94	1.04	1.02	1.14	1.02	1.14	1.06	0.93	1.05
Sb	1.42	2.01	1.84	1.69	1.99	3.59	1.81	1.54	4.35	2.5
Mn	500	570	550	470	635	510	570	565	540	520
Na	7200	10400	12500	13500	11900	12700	12700	13000	12700	10700
K	14100	21300	24100	22100	20600	24400	21600	22900	21600	19100

Neutron Capture Gamma-Ray Analysis (Prompt Gamma Neutron Activation Analysis, PGNAA)

The neutron radiation method of analysis is based on the application of prompt gamma-ray spectrometry arising from neutron capture by atomic nuclei of chemical elements, i.e., the capture of neutrons accompanied by the simultaneous emission of gamma radiation [3].

The principal processes governing the interaction of slow neutrons with atomic nuclei are elastic scattering and radiative capture. In the energy range below 10 MeV, the interaction mechanism is predominantly characterized by neutron capture processes. Neutron capture leads to the formation of a compound nucleus in an excited state, with excitation energy determined by the following expression:

$$E^* = \frac{M}{M+m} E_n + B_n \quad (1)$$

where M is the mass of the formed (compound) nucleus, m is the mass of the neutron, B_n is the binding energy of the neutron in the compound nucleus, and E_n is the kinetic energy of the neutron prior to interaction.

The excited nucleus transitions to a lower energy state through the emission of particles, gamma quanta, or via fission. This transition occurs after a characteristic time that is long compared to the nuclear timescale (~10^{-22} s). The mode of de-excitation does not depend on the mechanism by which the compound nucleus was formed; rather, it depends solely on its excitation energy.

The excitation energy (W) of the compound nucleus is given by:

$$W=\varepsilon_n+AE_n/(A+1) \quad (2)$$

where ε_n is the binding energy of the captured neutron in the compound nucleus, E_n is the kinetic energy of the neutron prior to capture, and A is the mass number of the nucleus.

The gamma-ray spectrum resulting from neutron capture, depending on the neutron binding energy (ε_n) in the product nucleus, spans a wide energy range-from approximately 0.1 MeV (e.g., for nuclei such as Mn, Fe, As, Nb, Ag, Sb, Cs, Eu, Hf, Ta) up to 10 MeV or higher (e.g., for nuclei such as B, N, Ti, V, Sr, Se, Ge).

Such a broad energy range makes it possible, in principle, to develop multi-element analytical methods based on prompt gamma-ray spectrometry of neutron capture. The sensitivity of the analysis depends on the intensity of the analytical gamma lines and their position within the spectrum, which determines the ability to distinguish them from the background and overlapping peaks.

The developed analytical methodologies for copper-molybdenum ores and related technological products allow, in addition to iron and copper, the simultaneous determination of potassium, sodium, manganese, chlorine, titanium, and aluminum from a single sample.

Table 3 presents the detection limits of several chemical elements determined in technogenic and environmental samples.

Table 3.

List of Elements Determined in Technogenic and Environmental Samples by Neutron Capture Gamma-Ray Spectrometry

Elements	Minimum Economic Grade, %	Limit of Detection, %	Elements	Minimum Economically Viable Concentration, %	Limit of Detection, %
Sodium	10	0.3	Manganese	2.5	0.05
Aluminum	10	0.7	Iron	25	0.16
Silicon	40	1.6	Cobalt	0.15	0.03
Sulfur	5	0.2	Nickel	0.25	0.1
Chlorine	20	0.008	Copper	0.7	0.14
Potassium	8	0.3	Arsenic	5	1
Calcium	20	0.7	Cadmium	0.1	0.003
Scandium	0.04	0.03	Samarium	0.02	0.009
Titanium	2	0.03	Gadolinium	0.01	0.0003
Vanadium	0.03	0.2	Mercury	0.1-1	0.005
Chromium	2	0.2			

As can be seen from the results presented in Table 3, the developed analytical methodologies for environmental and technogenic samples enable the simultaneous determination of potassium, sodium, manganese, chlorine, titanium, and aluminum within a single sample. A comparison of the detection limits with the minimum economically viable concentrations for each element is shown in Figure 2.

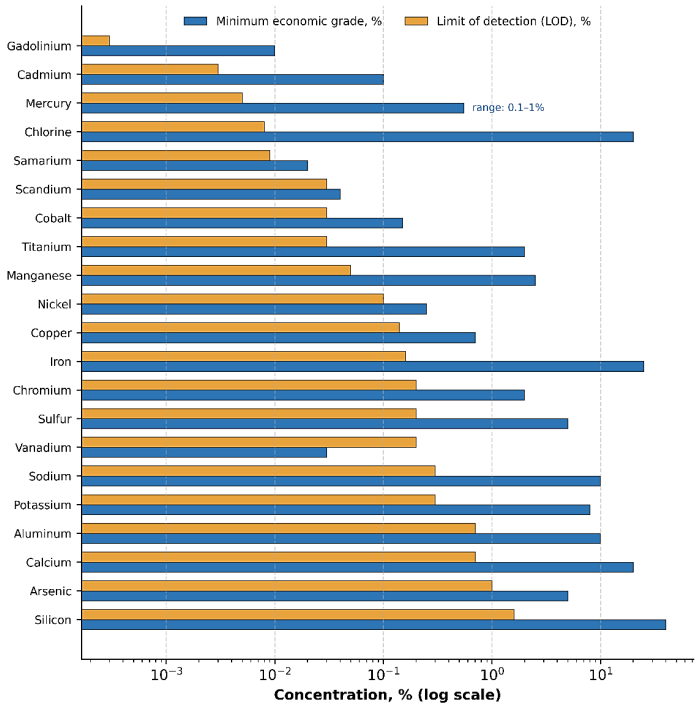

Figure 2. Limit of detection versus minimum economic grade for elements determined by neutron capture gamma-ray spectrometry (log scale)

Figure 2 demonstrates that the detection limits achieved are, for most elements, one to three orders of magnitude below the corresponding economic threshold, indicating sufficient analytical sensitivity for practical applications.

Gamma Activation Analysis (GAA)

A relatively less studied but promising method of elemental analysis is based on the use of gamma spectrometry of radiation generated in photonuclear reactions under the influence of bremsstrahlung radiation.

As a result of the interaction of gamma quanta with atomic nuclei via reactions of the type $X_A(\gamma, \gamma')X_A^m$, gamma-emitting isomeric states are formed [2, 4]. In certain elements with atomic mass greater than 33, such photonuclear reactions lead to the formation of isomers with sufficiently long half-lives.

The probability of photonuclear reactions leading to the formation of isomeric nuclei exhibits a threshold behavior. That is, for each atomic nucleus, such reactions occur only when the energy of the incident high-energy gamma quanta exceeds a specific threshold value.

The main nuclear-physical characteristics governing the formation of isomers (i.e., metastable nuclear states) and the corresponding analytical methods based on them include: the cross-section of the photonuclear reaction, the threshold energy required for the reaction, the half-life of the resulting isomer, and the yield and energy of the emitted gamma radiation.

Nuclear isomerism is determined by the structural features of atomic nuclei. Isomeric states arise when the transition of a nucleus to a lower energy state via gamma emission is hindered. Such isomers are particularly common in specific regions of mass numbers, often referred to as “islands of isomerism” ($A \approx 50, 82, 126$).

The threshold energy of the (γ, γ′) reaction is determined by the fundamental properties of atomic nuclei, primarily the nuclear charge and mass. An important role is also played by the gamma-ray yield and the intensity of the emitted radiation.

As the atomic number decreases, the threshold energy for the (γ, γ′) reaction generally increases, which can be exploited for the selective determination of specific elements. For practical applications of the (γ, γ′) reaction in elemental analysis, it is advisable to use gamma radiation with energies below 20 MeV.

According to literature data on gamma activation analysis, when the energy exceeds approximately 12 MeV, the variety of photonuclear reactions increases significantly. In addition to the (γ, γ′) reaction, other processes such as (γ, n), (γ, p), and (γ, f) reactions may occur. The presence of these additional reactions complicates the resulting gamma spectrum emitted by the sample, leading to difficulties in spectral identification and in accounting for the influence of interfering elements during analytical measurements.

The experimental studies in this work were carried out using a linear electron accelerator of the UELR-8-10A type, which produces bremsstrahlung radiation with a maximum energy of approximately 8.5 MeV.

Experimental Setup and Analytical Procedure for Gamma Activation Analysis

A relatively large sample mass of approximately 500 g was used. The experimental setup was designed with a vertical configuration. At a height of 12 meters, both the investigated and reference samples were weighed and then allowed to move vertically under the influence of gravity, stopping at the irradiation position where they were exposed to a bremsstrahlung beam with an energy of 8.5 MeV.

The irradiation time was selected based on the half-lives of the isomers formed in the investigated and reference samples as a result of photonuclear reactions. Experimental studies were carried out using model mixtures based on gold- and silver-bearing sulfide ore matrices with varying concentrations of Au, Ag, W, Y, and Re. These model mixtures were prepared by mixing known quantities of the target elements according to certified reference mixture preparation procedures. As a result, correlations were established between the intensity of gamma radiation emitted by metastable nuclei formed in photonuclear reactions and the concentration of the target elements in the model samples [10, 11].

The spectrometric system was based on a high-purity germanium (HPGe) semiconductor detector with an energy resolution of 1.7 keV at the 1333 keV gamma line of ^{60}Co. The gamma spectra were processed using the modern spectrometric software package Genie-2000.

Under irradiation with bremsstrahlung radiation of 8.5 MeV and photon flux densities in the range of 10^{13}–10^{15} photons/(cm²·s), photonuclear reactions leading to the excitation of isomeric states occur only in a limited number of elements, including yttrium (^{89}Y), gold (^{197}Au), silver (^{107},^{109}Ag), tungsten (^{183}W), and others.

Analysis of the gamma spectra of irradiated samples showed that the isomer ^{107m}Ag, with a half-life of 44.3 s, exhibits an analytical gamma line at 93.2 keV, while the isomer ^{109m}Ag, with a half-life of 39.6 s, has a gamma line at 88 keV.

As a result of the following photonuclear reactions, short-lived isomers of silver are formed:

^{107}Ag (γ, γ’) ^{107m}Ag; ^{109}Ag (γ, γ’) ^{109m}Ag (3)

Samples with known silver contents (reference materials) and unknown samples were irradiated sequentially, and the mass fraction of silver in the samples was determined using a relative method.

Taking into account the half-lives of the isomers ^{107m}Ag and ^{109m}Ag, the optimal analytical time regimes were calculated as follows: irradiation time $t_{(irr)}$ = 40 s, cooling time $t_{(cool)}$ = 2 s, and measurement time $t_{(meas)}$ = 38 s. The total time required for determining the silver content in a single sample was approximately 80 seconds.

Thus, based on the conducted studies evaluating the applicability of nuclear-physical methods for elemental analysis of technogenic and environmental samples, the effective analytical ranges and detection limits for the determined chemical elements were established.

Conclusion

The elemental composition of soils and plants collected from industrial and technogenic regions of Uzbekistan was investigated using instrumental neutron activation analysis (INAA). Certified reference materials, including IAEA-336 (Lichen) and NIST SRM 1572 (Citrus Leaves), were used to verify the accuracy and reliability of the analytical procedures. The comparison of experimental and certified values demonstrated good agreement and confirmed the validity of the developed methodologies.

The neutron-radiation analytical method was applied to ores and rocks, and its capabilities for the simultaneous determination of iron (Fe), copper (Cu), potassium (K), sodium (Na), manganese (Mn), chlorine (Cl), titanium (Ti), and aluminum (Al) were demonstrated. The obtained results indicate that neutron-based analytical techniques provide high sensitivity, multi-element determination, and low detection limits, making them suitable for environmental monitoring and technological process control.

In addition, the applicability of gamma activation analysis for determining the elemental composition of technogenic and environmental samples was evaluated. Based on the conducted studies, the analytical ranges and detection limits for a number of chemical elements were established. The results confirm that nuclear-physical analytical methods are effective tools for the investigation of environmental and technogenic objects and have significant potential for applications in ecological assessment, geological exploration, and mining-metallurgical industries.

References

1. Aripov G., Sirazhet Kh., Mamurov A., Tazhiev N.Yu. Neutron-radiation determination of some elements // Atomic energy. – 1978. – Vol. 45, No. 2. – P. 119–122.
2. Burmistenko Yu.N. Photonuclear analysis of the composition of matter. – M.: Energoatomizdat, 1986. – 200 P.
3. Guma V.I., Demidov A.M., Ivanov V.A., Miller V.V. Neutron radiation analysis. – M.: Energoatomizdat, 1984. – 64 P.
4. Danagulyan A.S., Oganesyan G.O., Bakhshiyan T.M., Avakyan R.O., Avetisyan A.E., Kerobyan I.A., Dallakyan R.K. Photonuclear reactions on nuclei ^{112}, ^{118}, ^{124}Sn, Te and Hf // Nuclear Physics. – 2014. – Vol. 77, No. 11. – P. 1378–1385.

5. Kist A.A. Phenomenology of biogeochemistry and bioinorganic chemistry. – Tashkent: Fan, 1987. – 236 P.
6. Kurbanov B.I. Prompt neutron capture gamma spectrometry for analytical applications. – Tashkent: Fan va tehnologiyalar nashriyot-matbaa uyi, 2021. – 212 P.
7. Frontasyeva M.V. Neutron activation analysis in life sciences // Physics of elementary particles and atomic nucleus. – 2011. – Vol. 42, No. 2. – P. 636–716.
8. Glascock M.D. An overview of neutron activation analysis. – Columbia, MO: University of Missouri Research Reactor (MURR). – 2006.
9. Greenberg R.R., Bode P., Fernandes E.A.D.N. Neutron activation analysis: A primary method of measurement // Spectrochimica Acta Part B: Atomic Spectroscopy. – 2011. – Vol. 66, No. 3–4. – P. 193–241.
10. Molnar G.L. (Ed.). Handbook of Prompt Gamma Activation Analysis with Neutron Beams. – Boston: Springer, 2004. – 424 P.
11. Szentmiklósi L. et al. Improved analytical workflow for prompt gamma activation analysis // Journal of Radioanalytical and Nuclear Chemistry. – 2024. – Vol. 333, No. 7. – P. 3325–3333.

ДЛЯ ЗАМЕТОК

ДЛЯ ЗАМЕТОК

UNIVERSUM: ТЕХНИЧЕСКИЕ НАУКИ

Электронный научный журнал

№ 9(150)
Сентябрь 2026 г.
Часть 8

Свидетельство о регистрации СМИ: ЭЛ № ФС 77 – 54434 от 17.06.2013

Издание содержит научную информацию и в соответствии с ч. 4 ст. 1 Федерального закона от 29.12.2010 № 436-ФЗ «О защите детей от информации, причиняющей вред их здоровью и развитию» не подлежит классификации (маркировке) по возрастным категориям

Издательство ООО «Юниверсум»

Объём издания: 68 с.

Минимальные системные требования: процессор с частотой от 1,3 ГГц; ОЗУ от 512 МБ; программа для чтения PDF-файлов; доступ к сети Интернет

Дата размещения в сети Интернет: 28.09.2206

Журнал размещается в:

CYBERLENINKA

Google scholar

BASE

OpenAIRE

НАУЧНАЯ ЭЛЕКТРОННАЯ БИБЛИОТЕКА eLIBRARY.RU

ULRICHSWEB GLOBAL SERIALS DIRECTORY

СОЦИОНЕТ

EBSCO

Registry of Open Access Repositories (ROAR)